Journal of Hydrology: Regional Studies 62 (2025) 102930

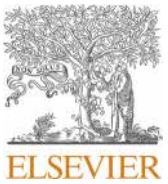

Contents lists available at ScienceDirect

Journal of Hydrology: Regional Studies

journal homepage: www.elsevier.com/locate/ejrh

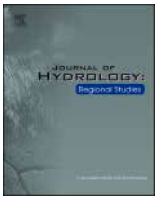

Drought feature assessment unravels how temperature increase has enhanced earlier and more severe drought in Lebanon over the last 60 years

Georgie Elias [a], Georgia Majdalani [a], Ghaleb Faour [b], Florent Mouillot [a,*]

[a] CEFE, Univ Montpellier, CNRS, EPHE, IRD, 1919 Route de Mende, Montpellier 34293 CEDEX 5, France
[b] National Center for Remote Sensing, National Council for Scientific Research (CNRS), Riad al Soloh, Beirut 1107 2260, Lebanon

ARTICLE INFO

Keywords:
Multifaceted drought
DFEAT
Drought trends
Onset
Offset
Duration
Severity
Middle-East
Lebanon

ABSTRACT

Study Region: Lebanon, Middle-East
Study Focus: While recent drought assessments predominantly rely on international meteorological indices, agro-environmental impacts are more closely linked to the diverse facets of drought derived from daily soil moisture depletion. This study investigates how recent climate change (1960–2020) has differentially affected drought facets in Lebanon. The DFEAT tool (Drought FEature Assessment Tool) was employed, which utilizes a daily soil water content time series derived from the empirical KBDI (Keetch-Byram Drought Index), to extract and analyze yearly trends in these drought facets, including onset/offset timings, duration, peak drought timing and severity value, and soil drying/rewetting rates.
New Hydrological Insights for the Region: A gradual shift toward drier conditions was revealed by the analysis, marked by a 5-day delay in drought offset and a significant earlier onset by 17 days. This trend emerges under annual precipitation stability but a seasonal redistribution, enhanced by rising temperatures. These changes have resulted in more prolonged drought episodes, extending by 15 days over the coastal areas and becoming more pronounced in the arid eastern regions of the country. Additionally, an increase in peak drought severity by 3 mm, a marginal rise in soil moisture drying rates by 0.096 mm.day^{-1}, and a total reduction in the intensity of autumnal rainfall pulses by 10 mm were observed. The escalating drier pattern underscores the need for adaptive management strategies in Lebanon's drought-prone sectors.

1. Introduction

Drought exerts profound impacts on terrestrial ecosystems functioning, as well as on society and economy across diverse hydro-climatic regions worldwide (Mishra and Singh, 2010; Wilhite, 2016). Drought is commonly defined as an abnormal deficiency in water supply (compared to normal values) extending over a significant period and region (Koutroulis et al., 2011; Slette et al., 2019). In general, the initial impacts of drought originating from anomalous meteorological conditions (i.e., meteorological drought) are typically manifested in agriculture (i.e., agricultural drought), which is highly sensitive to soil moisture depletion driven by increased evapotranspiration. In contrast, surface and subsurface water resources (i.e., hydrological drought) are often the last to be significantly

* Corresponding author.
E-mail addresses: georgie.elias@cefe.cnrs.fr (G. Elias), florent.mouillot@ird.fr (F. Mouillot).

https://doi.org/10.1016/j.ejrh.2025.102930
Received 9 March 2025; Received in revised form 31 October 2025; Accepted 7 November 2025
Available online 11 November 2025

affected if prolonged dry periods persist (Minea and Albulescu, 2025; Wilhite and Glantz, 1985; Yihdego et al., 2019).

Globally, the intensification of drought characteristics over the last decades, primarily duration and severity, has been mostly attributed to changes in key climatic drivers, such as precipitation and temperature, resulting from increased greenhouse gas emissions (Dai, 2013; Dai et al., 2004; Gounmene et al., 2025; Řehoř et al., 2023; Vicente-Serrano et al., 2022; Zhu et al., 2024). This intensification is projected to continue throughout this century (Amin et al., 2025; Dong et al., 2022), particularly in climate-vulnerable regions like the Mediterranean Basin (MB) (Collins et al., 2013; Tramblay et al., 2020). Notably, the MB and especially its eastern part (Middle-East), have already experienced increases in both the severity and duration of droughts since the mid to late 20th century (Cook et al., 2016; Mathbout et al., 2021, 2018; Sousa et al., 2011; Tsesmelis et al., 2023; Vicente-Serrano et al., 2014).This trend is attributable in part to the region's warming, which has been occurring at a faster rate than the global average since the 1980s (Azzopardi et al., 2020; Zittis et al., 2022).

These drought events are projected to become more severe and frequent due to anticipated reductions in precipitation and risings in temperatures (Dubrovský et al., 2014; Essa et al., 2023; Hertig and Tramblay, 2017; Mathbout et al., 2023; Politi et al., 2022), leading the region to be classified as a prominent regional climate change hotspot (Cos et al., 2022; Lionello and Scarascia, 2018; Tuel and Eltahir, 2020; Xu et al., 2019). This escalating trend is especially critical for the Middle-East region, where chronic water scarcity, high socio-economic vulnerability, and limited adaptive capacity amplify risks (Al-Rimmawi, 2012; Mfarrej, 2025; Waha et al., 2017). As a recognized climate change hotspot, the region faces pressures on agro-ecosystems (Elias et al., 2025), making it a vital focus for drought research (Sakellariou et al., 2024; Tramblay et al., 2020).

Already, recent evidence from the region has highlighted the negative implications of drought on rainfed agriculture (Elias et al., 2025; Páscoa et al., 2017; Ribeiro et al., 2019), wildfire hazards in grasslands and forests (Majdalani et al., 2022; Ruffault et al., 2023; Russo et al., 2017; Turco et al., 2017), limitations on tree growth (Elias et al., 2025; Lempereur et al., 2017, 2015; Rambal et al., 2014), and increased tree mortality (Camarero et al., 2015; Choat et al., 2018; Valeriano et al., 2021). The convergence of these drought-related threats may exceed the capacity of developing countries, particularly those in the Middle-East, to effectively mitigate or manage the impacts of severe drought episodes (Miyan, 2015). This underscores the need for evidence on ongoing drought trends to better anticipate and warn of climate change impacts (Jomaa et al., 2024).

To date, the majority of studies examining spatiotemporal drought trends within the MB have relied on the application of well-established and highly recognized drought indices: the Standardized Precipitation Index (SPI; McKee et al., 1993), based on probabilistic approach for precipitation to evaluate meteorological droughts and the Standardized Precipitation Evapotranspiration Index (SPEI; Vicente-Serrano et al., 2010), which combines sensitivity to changes in evaporative demand with the simplicity of calculation and the multi-temporal nature of the SPI. The use of both standardized indices in hydro-meteorological drought trend studies has been appealing due to their limited climatic data requirements and straightforward calculation process, covering various drought types based on different accumulation periods (i.e., multi-scalar characteristic) (Gounmene et al., 2025; Kesgin et al., 2024; Marcos-Garcia et al., 2017).

However, because these indices rely on monthly aggregated data, they may obscure short-term variability and sub-monthly fluctuations in precipitation and evaporative demand (Deo et al., 2017; Elias et al., 2024; Kim et al., 2009). This temporal smoothing might actually hide important climate signals that are critical for agro-environmental impact assessment (Ruffault et al., 2013; Tramblay et al., 2020). As a result, they are less effective at capturing rapid-onset or short-lived drought events, which play a decisive role in agricultural productivity and ecosystem functioning (Elias et al., 2025).

For instance, recent research highlights that variations in daily precipitation events, rather than monthly mean, are increasingly considered as potential significant climate change drivers of terrestrial functioning through partial soil refilling (Felton et al., 2021; Gherardi and Sala, 2015; Liu et al., 2020; Ritter et al., 2020; Zhang et al., 2021) when increasing dry spells and more extreme precipitation events increasingly co-occur (Deng et al., 2024). Similarly, drought timing (onset and offset) or duration, requiring short temporal time steps, are increasingly considered (Hahn et al., 2021; Keeley et al., 2022; Salesa et al., 2024; Wang et al., 2024). While these aspects are gaining recognition, they are still rarely evaluated using daily data (Deo et al., 2017; Elias et al., 2024; Ruffault et al., 2013). New drought features, such as soil desiccation speed during drought onset, have recently emerged as an underappreciated climate change signal (Liu et al., 2024b; Walker and Van Loon, 2023) leading to impactful flash drought (Yuan et al., 2023; Zeng et al., 2023).

In turn, drought trend assessments could benefit of being considered as a multifaceted phenomenon, characterized by different uncorrelated and impactful features, until now hidden in temporally buffered indices (Elias et al., 2024; Jeong et al., 2024; Martins Careto et al., 2024; Onyutha, 2017; Ruffault et al., 2013), leading to an underestimation of their impact (Liu et al 2024a).

To reach this goal, we applied the DFEAT tool (Drought FEature Assessment Tool; Elias et al., 2024), a recently developed automated algorithm that converts daily soil water content time series into comprehensive yearly drought facets (Elias et al., 2024). Despite acknowledged warnings on model discrepancies in characterizing drought (Gu et al., 2019), DFEAT was applied on a targeted single, yet widely recognized daily drought index, the Keetch-Byram Drought Index (KBDI; Keetch and Byram, 1968). It is hypothesized that the DFEAT approach will offer key novel insights into spatiotemporal drought trends under Mediterranean conditions, as viewed through a diverse set of features including onset, offset, duration, drying rate, peak drought days and severity, and mean rainfall pulses intensity, previously identified as driving most agro-ecoystems functioning in the region (Elias et al., 2025), and thus limiting interpretations to identified processes.

As a first application of DFEAT in operational drought trend monitoring, the objectives here are to 1) investigate recent spatiotemporal trends in seven key drought features from 1960 to 2020 across Lebanon and 2) explore how a common regional trend in climatic variables (air temperature and precipitation) can differentially affect key aspects of seasonal drought, thus, potentially revisiting the previous assessments only based on precipitation amount or standard anomalies.

2. Materials and methods

2.1. Study Area

The study area covers Lebanon (Fig. 1), a Mediterranean drought-prone country, spanning 10452 km^2 and hosting a population of 6 million people. Located between 33°–35°N and 35°–37°E on the eastern shore of the Mediterranean Sea, Lebanon's climate is characterized by a typical Mediterranean pattern with four distinct seasons: moderately cold and rainy winters, warm and dry summers, and mild springs and autumns (Halwani and Halwani, 2022; Kobrossi et al., 2021). Lebanon has numerous rivers (fourteen in total) and thousands of springs scattered across its territory (Shaban, 2020), ensuring irrigation plans for agriculture.

The country has a very diverse topography that divide its territory into three major geomorphological features: Mount-Lebanon and Anti-Lebanon mountainous chains laying parallel to the Mediterranean Sea, separated by the Bekaa valley which contains the largest cultivated land in the country by surface area and productive volume, ensuring the food security of Lebanon (Verner et al., 2018). This topography creates a climatic barrier that captures wet air masses blown by wind from the Mediterranean Sea, resulting in Lebanon's relatively high precipitation levels, including both rainfall and snow (Jomaa et al., 2019). As a result of this rugged topography, the precipitation is unevenly distributed over the country during the wet periods of the year (October to March), with January and December receiving the highest annual amounts (Kobrossi et al., 2021; Shaban, 2020). This variability defines numerous microclimatic zones along the country's aridity gradient, where sub-humid conditions prevail over the coastal Mediterranean areas (800–1000 mm) and humid patterns dominate over Mount-Lebanon receiving more than 1000 mm of annual precipitations. However, moving eastward, the precipitation gradient decreases sharply becoming more pronounced over the eastern and north-eastern arid regions, particularly from the Bekaa valley toward the Syrian border, where the annual precipitation ranges between 200 and 600 mm (Shaban et al., 2019; Shaban and Houhou, 2015; Verner et al., 2018). Lebanon's climate is also marked by prolonged warm and dry summers, extending from June to October, which leads to seasonal summer drought with September typically being the driest month of the year (Kobrossi et al., 2021).

2.2. Drought features extraction from the daily KBDI time series

At the national scale for Lebanon, DFEAT (Elias et al., 2024) was used to extract a comprehensive set of yearly drought features from the daily calculated KBDI (Keetch and Byram, 1968) time series over the hydrological years from 1960 through 2020.

2.2.1. Keetch-Byram Drought Index calculation (KBDI)

The Keetch-Byram Drought Index (KBDI; Keetch and Byram, 1968) is an empirical, cumulative soil moisture drought index, calculated as the balance between effective rainfall replenishing the soil (input) and empirical equations that approximate soil water

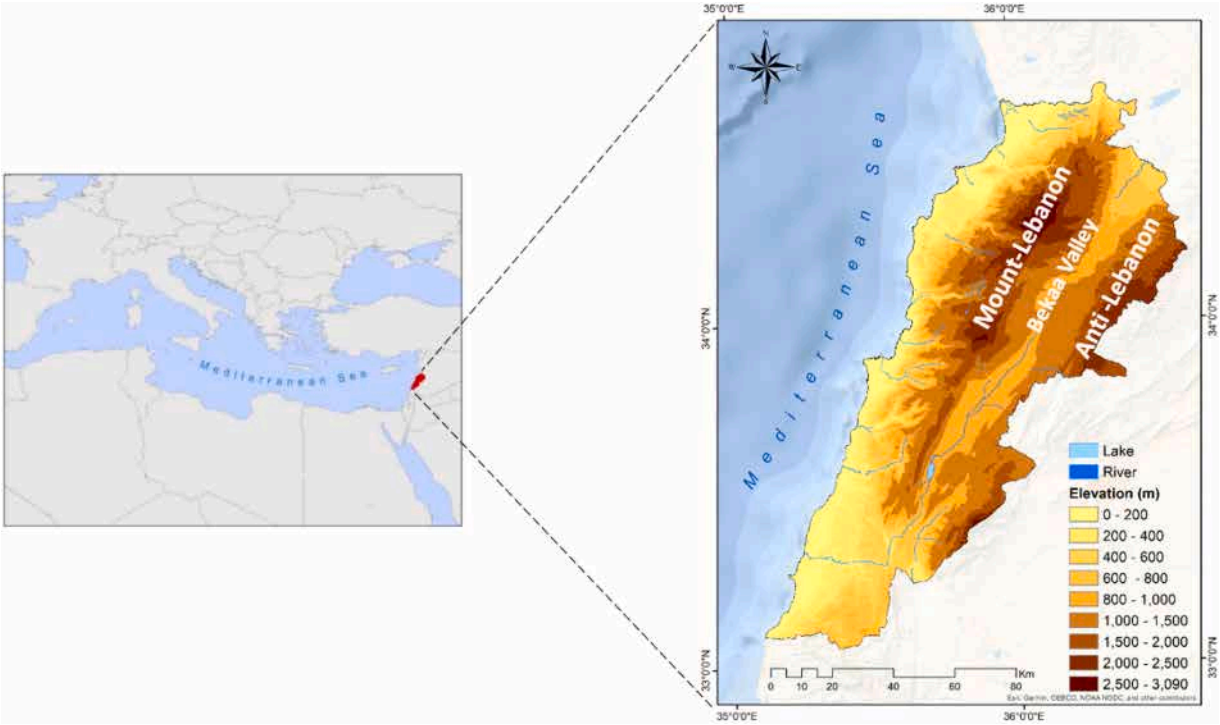

Fig. 1. Geographic map of Lebanon featuring elevations, river networks, and its location within the Mediterranean basin.

losses or actual evapotranspiration based on daily soil desiccation levels and a temperature-based evapotranspiration equation (output), and operates under the assumption of a maximum soil water holding capacity of 200 mm (Ganatsas et al., 2011; Häusler et al., 2019; Keetch and Byram, 1968).

First, effective rainfall (P_{net}) is estimated at the portion of precipitation that contributes to soil water recharge. To obtain P_{net}, 0.2 in. (or 5 mm) is subtracted from any daily rainfall amount exceeding this threshold, while rainfall below 0.2 in. is considered ineffective and set to zero (Eq. 1).

$$P_{net} = \max(0, \quad P_t - 0.2) \tag{1}$$

Next, the intermediate variable Q_t is calculated as the previous day's KBDI ($KBDI_{t-1}$) reduced by today effective rainfall (Eq. 2). Q_t therefore, represents the soil moisture deficit carried over from the previous day after accounting for today precipitation inputs, if any.

$$Q_t = (KBDI_{t-1}) - P_{net} \tag{2}$$

Subsequently, the daily soil water depletion also known as drought increment (dQ) is computed using an empirical temperature-based evapotranspiration function, which estimates soil water losses due to desiccation (Eq. 3), and considering a maximum soil water holding capacity of 8 in. (equivalent to 200 mm). It is expressed as:

$$dQ = \frac{10^{-3} \quad (800 \quad - Q_t)(0.968e^{0.0486T} \quad - 8.3)dt}{1 + 10.88e^{-0.0441R}} \tag{3}$$

where T is the daily maximum air temperature (in F°) at 2 m above the ground, R is the mean annual rainfall (inches), and dt is a time increment set equal to one day.

Finally, the $KBDI_t$ for the current day is derived by updating Q_t with the daily estimated soil water depletion (dQ), while constraining the index within its theoretical bounds of 0 (soil saturated at field capacity) and value approaching 800 indicate complete soil desiccation (maximum drought severity) (Eq. 4).

$$KBDI_t = \quad Q_t + dQ \tag{4}$$

This initial equation was then further converted by Crane (1982), to international units with air temperature in degrees Celsius (°C) and rainfall in millimeters (mm). The daily change in drought factor (dQ), measured in mm, is then expressed as shown in Eq. (5). Within this transformation, a KBDI value of 0 corresponds always to soil at field capacity, while the upper bound of 200 represents the maximum drought severity.

$$dQ = \frac{10^{-3}(203.2 - Q_t)(0.968e^{0.0875T+1.5552} - 8.3)dt}{1 + 10.88e^{-0.001736R}} \tag{5}$$

A modified version of the index (Eq. 6) was proposed by Ganatsas et al. (2011), by adapting daily maximum air temperature variable and the mean annual rainfall to adjust KBDI to Mediterranean conditions. This entails adjusting $KBDI_t$ calculations to also account for a reduction from 5 mm to 3 mm when computing net rainfall (P_{net}).

$$dQ = \frac{10^{-3}(200 - Q_t)(1.713e^{0.0875T+1.5552} - 14.59)dt}{1 + 10.88e^{-0.001736R}} \tag{6}$$

Compared to other soil moisture indices or process-based models, which often rely on numerous input parameters, calibration steps, and complex modeling assumptions (Granier et al., 1999; Mouillot et al., 2001), the KBDI offers significant practical advantages. It is cumulative, conceptually straightforward, and can be computed directly from widely available daily air temperature and precipitation data (Keetch and Byram, 1968). Its simplicity and minimal data requirements make it particularly suitable for long-term large-scale drought monitoring and for use within tools like DFEAT, also enabling broader regional applications (Elias et al., 2024).

In addition, the KBDI index has been used in Lebanon for investigating the drought-related seasonality of fire hazard (Hamadeh et al., 2017; Mitri et al., 2014). Its reliability has also been demonstrated in several Mediterranean countries, where it effectively reproduces the seasonal dynamics of live fuel moisture for various shrub species (Pellizzaro et al., 2007; Ruffault et al., 2018). Given this proven relevance in Mediterranean climates, the DFEAT tool (Elias et al., 2024) was developed and standardized specifically using the Mediterranean-adapted version of the KBDI (Ganatsas et al., 2011).

2.2.2. Meteorological data

For index calculation, the daily air temperature at 2 m and the total precipitation were downloaded from ERA5-Land datasets for Lebanon, featuring a spatial resolution of 9 km (Muñoz-Sabater et al., 2021). Although finer-scale datasets exist (≤1 km) (Fick and Hijmans, 2017; Karger et al., 2017), ERA5-Land was selected for this study due to several critical advantages related to its consistency, robustness, and temporal coverage (Muñoz-Sabater et al., 2021).

ERA5-Land is produced by the European Centre for Medium-Range Weather Forecasts (ECMWF) through advanced data assimilation techniques, combining global observations with state-of-the-art numerical weather prediction models (Muñoz-Sabater et al., 2021). This process ensures physically consistent fields of precipitation and temperature across time and space, which is particularly valuable in regions like Lebanon, where meteorological station data are sparse, unevenly distributed, and often discontinuous (Shaban et al., 2019; Shaban and Houhou, 2015). Compared to national meteorological networks that suffer from large temporal gaps and accessibility issues, ERA5-Land provides a continuous and homogeneous dataset from 1950 to the present, allowing for the

reconstruction of long-term drought features at the national scale (Aboelnour et al., 2025; Aschale et al., 2024; Ernst et al., 2025; Keune et al., 2025; Muñoz-Sabater et al., 2021). While its 9 km resolution provides ~130 grid cells for Lebanon's territory (10452 km^2), this resolution strikes a balance between computational feasibility for multi-decadal drought analyses and the spatiotemporal consistency required for robust trend detection (Ceppi et al., 2025; Gomis-Cebolla et al., 2023). Finer-resolution products (e.g., 1 km downscaled datasets) often lack the multi-decadal temporal span and rely on statistical downscaling methods, thus integrating coarser resolution trends similar to ER5-Land. This artificial finer resolution is not relevant for our regional study over the Lebanese climate gradient, not targeting specific fine grained application (Li et al., 2025; Zhang et al., 2024).

Accordingly, ERA5-Land represents the most suitable dataset for the aims of this study, offering a long-term, spatially consistent, and scientifically validated foundation for KBDI computation and the extraction of spatiotemporal drought features (Gatien et al., 2023; Ullah et al., 2024).

2.2.3. *DFEAT-Based extraction of yearly drought features*

After calculating the daily KBDI time series at the ERA5-Land 9 km spatial resolution over the 60-year study period, DFEAT tool extracts yearly drought features for each hydrological year (Elias et al., 2024) from the daily KBDI time series, based on critical soil desiccation thresholds that influence agro-ecosystem functioning (Elias et al., 2025).

These thresholds were chosen as they represent different drought levels, namely the low, moderate, and extreme drought levels, representing soil moisture reaching 25 %, 50 %, and 75 % of the total available water content (set to 200 mm), respectively (Elias et al., 2024). The 25 % threshold (or KBDI-50) was considered as an index of full soil profile refilling. This threshold was used to detect Multi-Year Droughts (MYD) occurring without winter soil deep drainage, which is a key factor in ground water recharge (Reinecke et al., 2021). The 50 % (KBDI-100) and 75 % (KBDI-150) thresholds correspond to the moderate and maximum critical thresholds of plant water stress identified across biomes globally (Fu et al., 2024), respectively. Also, both thresholds affect vegetation functioning through stomatal closure and subsequent plant transpiration and carbon assimilation (Granier et al., 1999), or tree growth through the disruption of cell turgescence in Mediterranean forests (Lempereur et al., 2017). The two thresholds were proposed to encompass various plant water use strategies (Klein, 2014) and soil textures (Saxton and Rawls, 2006). More drastic thresholds of 90 % are acknowledged as potentially of interest, but the high correlation between thresholds was illustrated by Elias et al. (2024).

Following DFEAT methodology, 19 yearly drought features/hydrological year could be characterized related to three drought onsets DOY (Day Of the Year), offsets DOY, duration (number of days between each considered onset and offset threshold), and severity (sum of water deficit, mm/day/year) for each considered soil desiccation level (Fig. 2). DFEAT also provides the peak drought timing for each hydrological year by determining the DOY when daily soil water depletion, as represented by the KBDI curve, reaches its maximum value. The corresponding severity value (peak KBDI), expressed in mm of water depletion and constrained to not exceed the fixed soil capacity of 200 mm, quantifies the intensity of the drought at that peak DOY. In addition, the daily maximum rates of soil moisture drying and rewetting (mm/day) were calculated using DFEAT. The drying rate represents the maximum daily soil water loss and is derived as the slope of the tangent to the drying curve (representing soil moisture depletion or drought propagation phase),

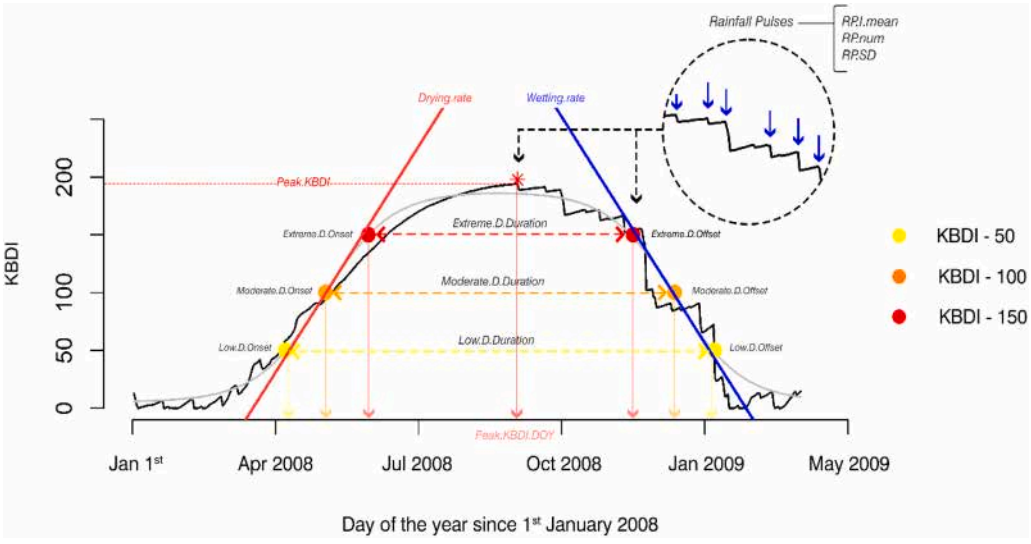

Fig. 2. Drought features derived from KBDI daily values (black line) of a hydrological year (from Day of the Year 1–420), across three soil desiccation thresholds: KBDI-50 in yellow, KBDI-100 in orange, and KBDI-150 in red, representing low, moderate, and extreme drought levels, respectively. Low.D.Duration: Low Drought Duration; Moderate.D.Duration: Moderate Drought Duration; Extreme.D.Duration: Extreme Drought Duration; Peak.KBDI.DOY: Day of the year featuring the highest KBDI value; Peak.KBDI: Peak KBDI Value; Extreme.D.Offset: Extreme Drought Offset; Low.D.Offset: Low Drought Offset; Moderate.D.Offset: Moderate Drought Offset; RP.I.mean: mean intensity of Rainfall Pulses; RP.num: Rainfall Pulses number; RP.SD: Rainfall Pulses Standard Deviation; Low.D.Onset: Low Drought Onset; Moderate.D.Onset: Moderate Drought Onset; Extreme.D.Onset: Extreme Drought Onset (Adapted from Elias et al. 2024).

while the wetting rate represents the maximum daily soil water recovery and is derived as the slope of the tangent to the wetting curve (representing soil moisture recharge or recovery phase) (Fig. 2). Additionally, DFEAT extracted the number, mean intensity (mm), and standard deviation of episodic rainfall pulses events occurring between the peak drought day of year (DOY) and the end of the extreme drought period at the end of the dry season (Elias et al., 2024).

The appeal of DFEAT utilization for drought monitoring and characterization lies in its ability to characterize these features over each considered hydrological year or even longer periods spanning consecutive hydrological years, defined in the earlier work of Elias et al. (2024) as Multi-Year Droughts (MYD), commonly observed in semi-arid and arid climates receiving lower annual amount of precipitation. These MYD events can last for several years or even decades without necessarily reaching one or more soil desiccation threshold for delimiting the end of that dry period.

Drawing up on this, the following uncorrelated specificities among the 19 extracted features have been retained, as earlier suggested by Elias et al. (2024): moderate drought duration, onset, offset, peak drought day (Peak KBDI DOY) and its severity value (Peak KBDI), soil moisture drying rates, and rainfall pulses mean intensity further used in the study for spatiotemporal drought facets trend analysis as integrative of climate variability.

2.3. *Statistical analyses: Trend detection and magnitude estimation*

To assess drought trends over the period 1960–2020, a nationwide pixel-based assessment was conducted on the previously retained drought features, alongside two key climatic parameters: annual aggregated mean air temperature and precipitation. Monotonic trends were tested with the non-parametric Mann-Kendall test (Kendall, 1975; Mann, 1945), implemented through the *MannKendall* function of the Kendall R package (McLeod, 2005). The magnitude of these trends was quantified using the Theil-Sen slope estimator (Sen, 1968), as implemented in the openair R package via the *TheilSen* function, which employs a bootstrap approach to estimate confidence intervals (Carslaw and Ropkins, 2012).

The non-parametric Mann-Kendall trend test is a robust and distribution-free statistical method that does not require prior knowledge of the parent distribution and is widely recognized as an efficient tool for detecting trends in drought features and climatic variables (Caloiero et al., 2018; Coscarelli et al., 2023; Koutsias et al., 2012; Richardson et al., 2022). In this study, trends were considered significant when p-values are lower than 0.1 (p-value < 0.1; 90 % confidence interval). Simultaneously, the Theil-Sen slope estimator selects the median slope from all lines formed by pairs of two-dimensional sample points. This method can offer significantly greater accuracy than ordinary least squares regression, particularly in the presence of skewed or heteroscedastic data (Alexander et al., 2006; Aschale et al., 2024; Caloiero et al., 2019; Ruffault et al., 2013).

A recent study on drought trends in Lebanon by Jomaa et al. (2024) revealed an increasing trend in drought severity over the last 30 years (1990–2021) and particularly since 1990, as assessed by mean of the SPI drought index. Consequently, in addition to analyzing spatiotemporal drought patterns over the entire 60-year period, the dataset was also divided into two sub-periods of 30-year intervals: pre-1990 (1960–1989) and post-1990 (1990–2019). To better assess this 1990 breakpoint year, we performed a piecewise regression

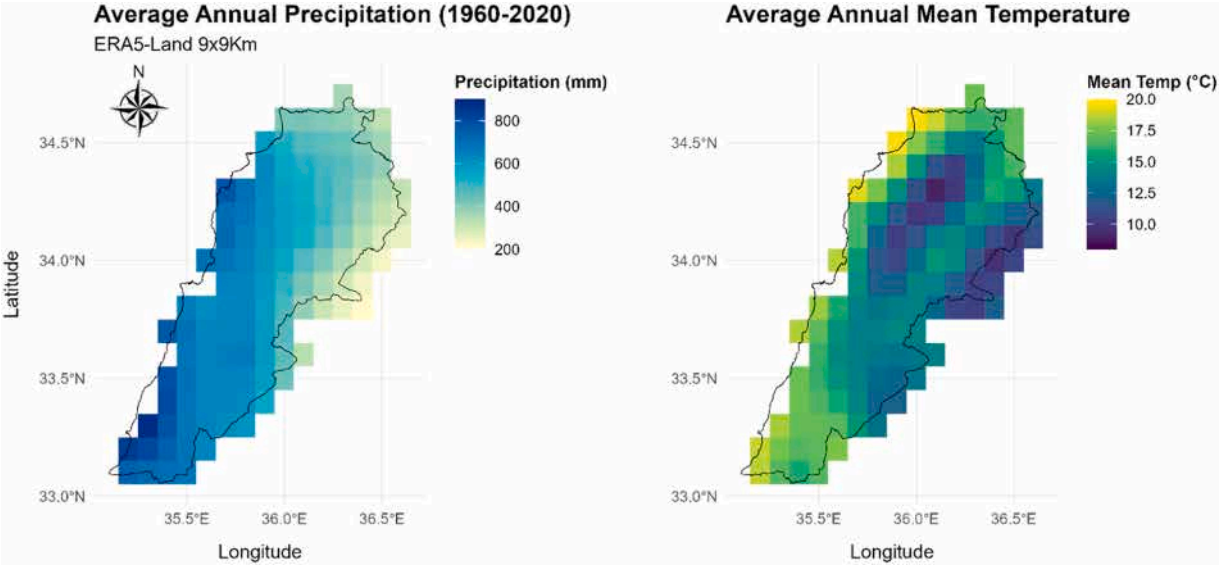

Fig. 3. Spatial distribution of average annual precipitation (mm) and mean air temperature (°C) across Lebanon for the period 1960–2020, based on ERA5-Land data at a 9 km pixel resolution. The left map represents the average annual precipitation, ranging from higher values (dark blue) to lower values (light yellow). The right map represents the distribution of average mean air temperature, where lower values appear in dark purple and higher values in yellow.

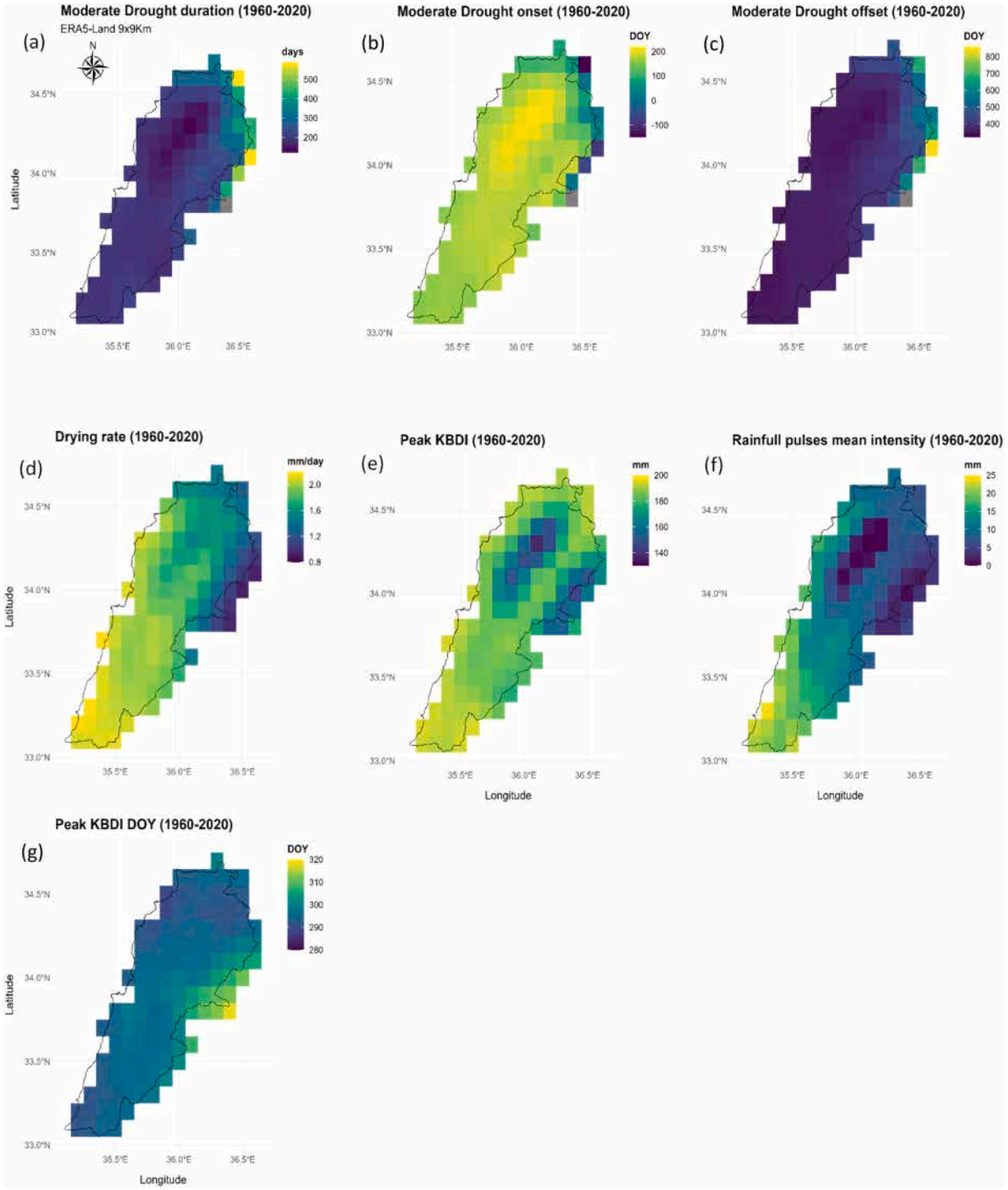

Fig. 4. Spatial distribution of the annual average of key drought features across Lebanon for the period 1960–2020, based on ERA5-Land data at a 9 km pixel resolution. The seven maps (a-g) are in different units (days, DOY, mm/day, and mm), and represent the average distribution of these features, where lower average values are shown in dark purple and higher values in yellow.

test, with varying breakpoint years from 1965 to 2015 (*lm* function R for linear regression), and retained which breakpoint year provided the minimum residual. Depending on the variable (onset or peak KBDI) and the pixel, we obtained breakpoint years varying between 1978 and 1990, with a median value around 1985. To ensure consistency, across regions, we kept the maximum value of 1990 for all analysis, in accordance with previous studies and providing a similar timeframe of 30 years before and after the break point.

3. Results

3.1. Spatial patterns of annual precipitation, mean air temperature, and key drought features across Lebanon (1960–2020)

The precipitation pattern across Lebanon reflects a west-east gradient following the country's rugged topography (Fig. 3). The average annual precipitation reaches approximately 900 mm in the southern coastal areas near the Mediterranean Sea for the period 1960–2020, and gradually decreases moving eastward toward the inland regions, reaching as low as 250 mm in the arid eastern parts. Similarly, the mountainous regions of Mount-Lebanon (west) and Anti-Lebanon (east) experience the lowest annual mean air temperatures, averaging around 8–10°C, while the average for the inland area between these mountains is 15°C. In contrast, the coastal areas record the highest mean annual air temperatures for that period, averaging around 20°C.

Fig. 4(a to g) illustrates how the precipitation and air temperature gradients transfer into yearly drought features at the 9 km pixel-based resolution of ERA5-Land.

Starting with drought duration (Fig. 4a), the coastal areas of Lebanon experience a duration ranging from 180 to 200 days, reflecting the relatively mild climatic conditions. The western mountain chains exhibit shorter drought duration, typically between 120 and 140 days. Moving eastward to the Bekaa valley which experiences a semi-arid climate, drought duration increases slightly, averaging around 220–250 days. This pattern intensifies further in the arid eastern regions near the Syrian border, where drought duration can reach as high as 600 days, surpassing the standard 365-day calendar year, and thus witnessing MYD pattern.

A similar west-to-east gradient is observed in the timing of drought onset DOY (Fig. 4b), averaging between DOY 155 (June 4) and 170 (June 19) in the coastal regions. The average onset is delayed in the western mountain chains, occurring around DOY 205 (July 24) and 220 (August 8). In the Bekaa valley, drought onset tends to occur earlier, averaging between DOY 160 (June 9) and 180 (June 29). In contrast, in the eastern arid regions of the country, drought onset exhibits negative values, with an average occurrence of −150 reflecting the frequent occurrence of MYD and indicating that, for any given year n starting on January 1st, drought could typically begin during the early days of year $n - 1$. Regarding drought offset timing (Fig. 4c), a regional pattern is observed, with annual average offsets occurring between DOY 340 (December 6, year n) and 355 (December 26, year n) in the sub-humid coastal areas and western mountains. In the Bekaa valley and further east, the offset begins to extend, ending within the DOY range of 380 (January 15, year $n + 1$) to 420 (February 24, year $n + 1$). However, in the arid eastern regions, drought offsets can extend significantly, reaching approximately DOY 800 which reflects an average offset occurring two years (i.e., in year $n + 2$) after the initiation of drought in year n.

Regarding the average annual soil moisture drying rate (Fig. 4d) and the peak KBDI severity (Fig. 4e), coastal areas exhibit the highest annual average soil moisture drying rates, ranging from 2.0 to 2.15 mm/day, while peak KBDI values fluctuate between 184 and 194 mm, establishing them as the highest in the country. In contrast, both features display slightly reduced values in the western mountainous chains where the average annual soil moisture drying rate falls between 1.5 and 1.7 mm/day, and the peak KBDI value ranges between 137 and 150 mm. In the Bekaa valley, the average drying rate experiences higher values, averaging between 1.65 and

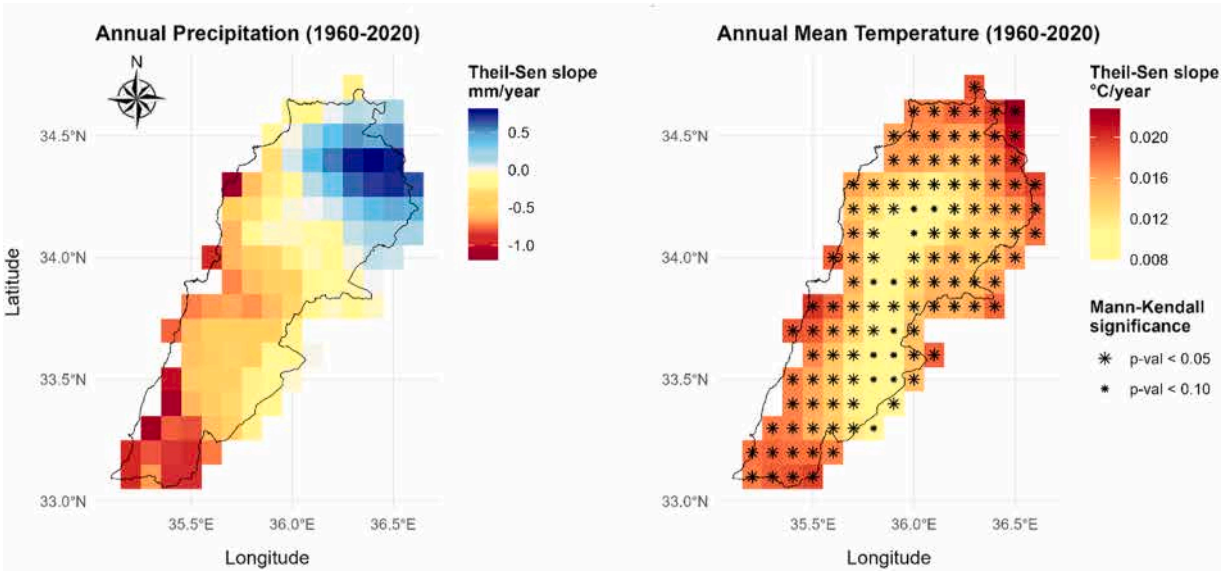

Fig. 5. Spatial distribution of the temporal trend of key climatic variables across Lebanon from 1960 to 2020. The left map illustrates trends in annual precipitation, while the right map shows changes in annual mean air temperature. Slopes are estimated using the Theil-Sen method, with small asterisks (*) indicating p-values less than 0.10 and larger asterisks (*) signifying p-values less than 0.05, based on the Mann-Kendall significance test. The absence of a symbol means that there is no statistically significant trend detected. Changes in climatic conditions are represented by a color gradient ranging from light yellow to dark red indicating either a decrease in precipitation or an increase in air temperature, while shades of blue indicate an increase in precipitation patterns or a decrease in air temperature.

1.85 mm/day, with peak KBDI severity values attaining higher levels between 170 and 180 mm. Ultimately, both features reach their lowest values in the eastern arid regions of the country, recording an average annual drying rate of 0.8 mm/day and a maximum peak drought severity of 140 mm, although belonging to the less rainfed region but experiencing the coldest temperatures. The timing of this peak drought severity occurs between DOY 290 (October 17) and 295 (October 22), across the country and reach an average DOY of 320 (November 16) in the most arid region.

Considering the episodic rainfall pulses that occur at the end of the dry season (Fig. 4f), both mountain chains exhibit an average close to zero, indicating nearly no rainfall pulses during the dry season at these altitudes. In contrast, the coastal areas experience the highest average annual intensity of rainfall pulses over the country, ranging from 15 to 25 mm. However, the semi-arid Bekaa region

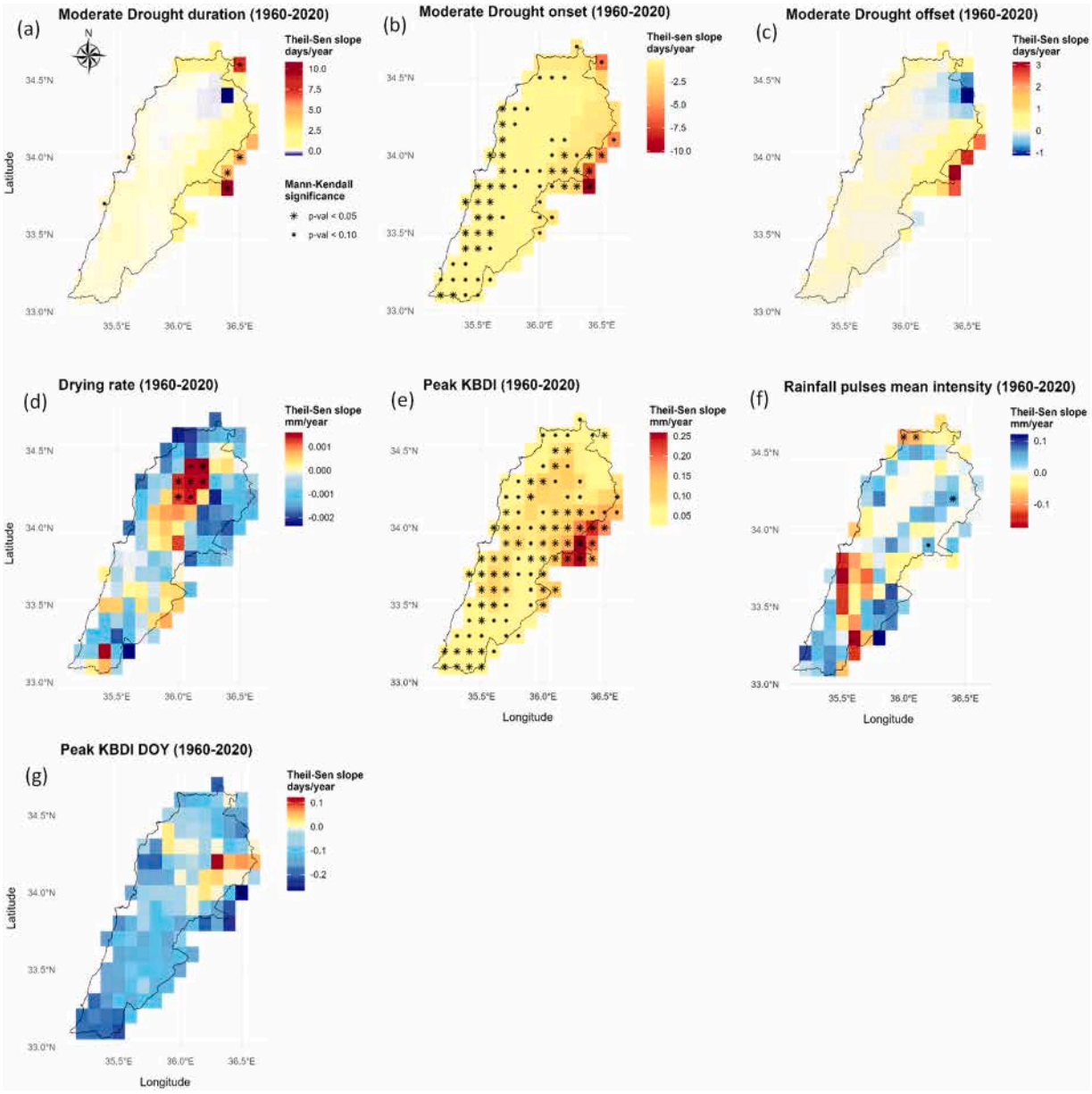

Fig. 6. Spatial distribution of Theil-Sen estimated slopes for the considered drought features (a-g) all over Lebanon during the period 1960–2020. Small asterisks (*) indicate p-values less than 0.10, while larger asterisks (*) signify p-values less than 0.05, as determined by the Mann-Kendall significance test. The absence of a symbol means that there is no statistically significant trend detected. Changes in drought conditions are directly reflected in the color gradient. A color gradient ranging from light yellow to dark red signifies an intensification of drought conditions (e.g., longer duration, earlier onset, delayed offset, higher peak severity, faster drying rate, and fewer rainfall pulses). In contrast, shades of blue indicate a decrease in drought conditions (e.g., shorter duration, delayed onset, earlier offset, lower peak severity, slower drying rate, and more rainfall pulses).

receives significantly lower rainfall pulse intensities averaging between 6 and 10 mm.

3.2. Spatiotemporal trend of annual precipitation, air temperature, and key drought facets over the last six decades (1960–2020)

The time course of the annual precipitation in Lebanon (1960–2020) reveals an overall decreasing (yet not significant) trend across most of the country with a more pronounced decline observed along the coastal areas, reaching −70 mm (-1.16 mm/year) over the 60-year period (Fig. 5). By contrast, certain regions in the north and the northeast have exhibited an increasing (non-significant) precipitation trend ranging from + 6 to + 48 mm. It is noteworthy that these areas generally experience semi-arid and arid climatic conditions and receive low annual rainfall averaging approximately at 250 mm (cf Fig. 3). Among the regions with the most important annual decrease in the south of the country, summer rainfall (June to August) experienced no significant trend (Man-Kendall p-value>0.1), and spring precipitations (March to May) experienced a slight yet not significant (Man-Kendall p-value>0.05) trend, so that the seasonal pattern of precipitation was also considered as constant.

During the same period, the observed temporal trend of the annual mean air temperature showed a significant increase across all climatic zones. This trend is the most pronounced in the coastal areas and the eastern arid regions, with an overall rise of + 0.70°C (+0.012°C/year) to + 1.2°C (+0.02°C/year) over the past six decades. In contrast, the interior regions of the country, as well as the higher western mountains (Mount-Lebanon) exhibited a less significant increase with air temperatures rising by approximately + 0.5°C (+0.008°C/year) over the period 1960–2020 (Fig. 5).

These analyses of the two main climatic drivers of regional drought, precipitation and air temperature, conclude that although a decreasing trend in precipitation is observed across the country, it is not statistically significant. In contrast, rising temperatures are likely to influence potential evapotranspiration and thus, enhance soil moisture depletion. Subsequently, to better investigate changes in drought features over Lebanon, both key climatic parameters spatiotemporal trends observation were completed with a comprehensive analysis of multifaceted drought features trends in Lebanon over the past six decades (Fig. 6a-g).

As a major finding, no significant trends were detected in drought duration across most of the country (Fig. 6a), in line with results based on annual precipitation trends. Yet non-significant, an increase in drought duration of approximately + 15 days (+0.25 days/year) was observed along the coastal areas, relative to an average annual duration of 200 days. This trend becomes more pronounced in the eastern arid regions where drought duration extended by + 50 (+0.8 days/year) to + 135 days (+2.25 days/year) out of a mean value of 600 days due to more frequent and prolonged MYD events linked to prevailed arid conditions. Some northeastern areas showed, in contrast, a decrease in drought duration by approximately −30 days (-0.5 days/year) between 1960 and 2020, in line with the upward observed trends in precipitation.

This slight increase in drought duration is however associated with a significant earlier drought onset (Fig. 6b), particularly in the coastal zones and western mountains where onset occurred −7 (-0.12 days/year) to −17 (-0.28 days/year) days earlier over the period 1960–2020. The shift becomes more pronounced moving eastward, from the Bekaa valley toward the Syrian border, where the onset advanced by −40 (-0.6 days/year) to −150 days (-2.5 days/year), witnessing increasing MYD. On the contrary, no significant change in drought offset timing was detected (Fig. 6c). Yet, a very slight delay of around + 5 days (+0.08 days/year) was observed along the coastal line, with numerous pixels exhibiting negligible trends, becoming slightly more pronounced in some eastern arid parts. Notably, in line with the patterns observed for duration in response to precipitation trends, the northeastern regions experienced an earlier drought offset of up to −60 days (-1 days/year).

Alongside the earlier onset of drought episodes, more severe drought conditions were observed, as reflected by significantly higher peak KBDI values (corresponding to the highest soil water desiccation of the year), across most of the country and particularly over the humid western mountains of Mount-Lebanon. The severity has increased by around + 3 mm (+0.05 mm/year) over the coastal areas to + 15 mm (+0.25 mm/year) on the eastern arid parts. Additionally, the earlier drought onset appears closely linked to higher soil moisture depletion rates at the start of the dry season (drying rate) (Fig. 6d), more particularly significant over the humid western mountains (+0.0016 mm/year). However, certain areas, such as the coastal regions and parts of the northeast, show a slight tendency toward slower soil drying rates (downward pattern) although these trends remain statistically insignificant.

Finally, the observed delayed drought offset at the end of the dry season illustrates less early fall rainfall events (Fig. 6f) associated with reduced rainfall pulse intensity, particularly dominant in the southern coastal areas where rainfall pulses decreased by around −10 mm (-0.16 mm/year). However, higher rainfall pulses were observed in the mountainous regions and parts of the Bekaa valley. This result is associated with a slight tendency toward earlier peak KBDI timing (Fig. 6g) as a result of earlier fall/late summer rainfall events. Even though these shifts in peak drought occurrence are statistically insignificant, they range from −6 days (-0.1 days/year) to −16 days (-0.26 days/year) earlier across the country.

In conclusion, while no significant trends in annual rainfall amounts and drought duration have been observed across the country, more specific drought features have been significantly affected by recent climate change as a slight spring precipitation decrease but mostly enhanced by temperatures as the main changing driver.

3.3. Recent emerging drought trends during the period 1990–2019

Based on the year 1990 identified as a breakpoint in the temporal trend of drought features (cf Section 2.3), we computed the temporal trend over the 1960–1989 and 1990–2019 periods separately. In contrast to the relatively constant conditions observed during the early period of 1960–1989 with no significant changes for all drought facets (cf Appendix A), the more recent period of 1990–2019 exhibits a pronounced intensification of drought conditions across all examined features (Fig. 8a-g). To further substantiate the temporal dynamics of drought conditions and address the potential shift around 1990, the yearly time course of two selected

drought features, yearly drought onset and peak KBDI (Fig. 7a-b), were examined. These features were chosen as illustrative examples due to their previously demonstrated significance over the 60-year period (1960–2020). Complementary evidence was also obtained from the average shapes of the daily KBDI cycles for each 30-year sub-period (1960–1989 and 1990–2019) (Fig. 7c). The scatterplots of yearly values revealed contrasting trends before and after 1990 (Fig. 7a-b), with relatively stable drought conditions during 1960–1989 (in blue) followed by a marked intensification during 1990–2019 (in red), as well as distinct changes in the 30-year means of the considered features. For drought onset, the average during 1960–1989 was 161.3 ± 10.97, which shifted to an earlier occurrence by about six days in 1990–2019, with a mean of 155.73 ± 10.54 (Fig. 7a). However, the mean peak drought was 191.63 ± 2.63 during 1960–1989, increasing by approximately 2 mm of water deficit to an average of 193.38 ± 2.46 in the second period 1990–2019 (Fig. 7b). This temporal evidence is reinforced by the averaged KBDI time course (Fig. 7c), which displayed a delayed curve in the earlier period (1960–1989; blue curve) but a shift toward earlier onset and more severe drought conditions in the later period (1990–2019; red curve). Together, these complementary analyses provide robust support for the existence of a regime shift in drought dynamics around 1990, beyond what is captured by the spatial distribution of long-term trends alone.

However, the trends observed during 1990–2019 differ in both magnitude and statistical significance from the broader patterns observed over the entire study period (1960–2020). Yet, these differences remain limited for drought duration and offset as both features continue to show non-significant increasing trends in both the 1990–2019 and 1960–2020 timeframes. During 1990–2019, drought duration (Fig. 8a) showed a non-significant increase ranging from + 15 days (+0.5 days/year) in the coastal regions and between + 130 (+4.3 days/year) and + 900 days (+30 days/year) in the arid zones, doubling the annual trends observed over the 1960–2020 period. These last high values becoming significant but only observed in the arid zone, indicate a shift from predominantly single-year drought events to more frequent MYD occurrences. Similarly, the non-significant delay in drought offset during the same period (Fig. 8c) ranged from a 4-day delay in most coastal and inland areas to between + 45 (+1.5 days/year) and + 360 days (+12 days/year) in the arid regions.

Alongside, a less widespread statistically significant earlier occurrence of drought onset was observed during the more recent period (Fig. 8b) compared to the whole 1960–2020 period, mostly localized along the coastal areas. The onset ranged from −10 days earlier (-0.33 days/year) in the coastal regions to a more pronounced shift of up to −450 days (-15 days/year) in the eastern arid zones, 2–5 times higher as a yearly decrease than observed over the 1960–2020 period. This last drastic pattern of earlier occurrence mirrors the trends observed in drought duration and highlights the increasing prevalence of prolonged MYD events.

Additionally, a reduction in the statistical significance of peak KBDI values (Fig. 8e) and soil moisture drying rates (Fig. 8d) was observed for the 1990–2019 period. However, both features continue to exhibit an intensifying positive trend. Peak KBDI severity varies between + 3 mm (+0.1 mm/year) in the coastal areas and approximately + 15 mm (+0.5 mm/year) in the eastern arid zones, while drying rates increased by + 0.045 to + 0.15 mm over the 30-year period. Notably, the highest increase in soil moisture drying rates was recorded across the coastal and inland regions during 1990–2019 compared to the 1960–2020 timeframe where they are only significant over the western mountainous chain.

Regarding the timing of peak KBDI, their occurrences were significantly earlier during 1990–2019 compared to 1960–2020 (Fig. 8g), particularly in the southern coastal and inland regions, where values ranged from −9 days (-0.3 days/year) to −24 days (-0.8 days/year). Meanwhile, in contrast to the 1960–2020 period, the mean intensity of rainfall pulses during the more recent sub-period of

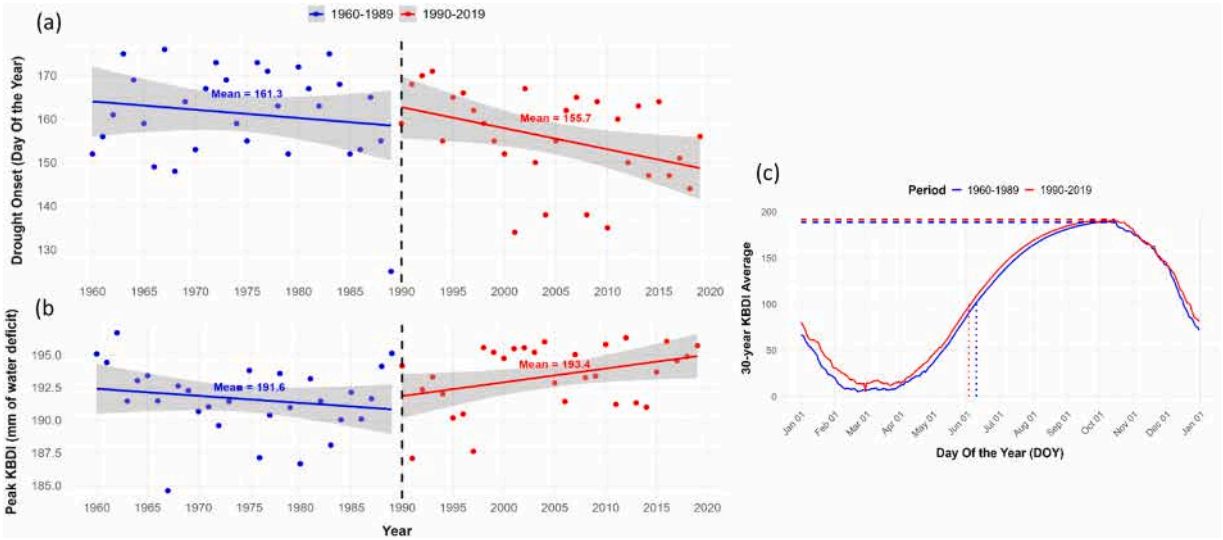

Fig. 7. Temporal time course of yearly drought onset (a) and yearly peak drought severity (b) during the two sub-periods, 1960–1989 (blue) and 1990–2019 (red), including the corresponding 30-year mean values. Panel (c) presents the averaged KBDI daily time course, highlighting differences between the earlier period (1960–1989; blue curve) and the more recent period (1990–2019; red curve).

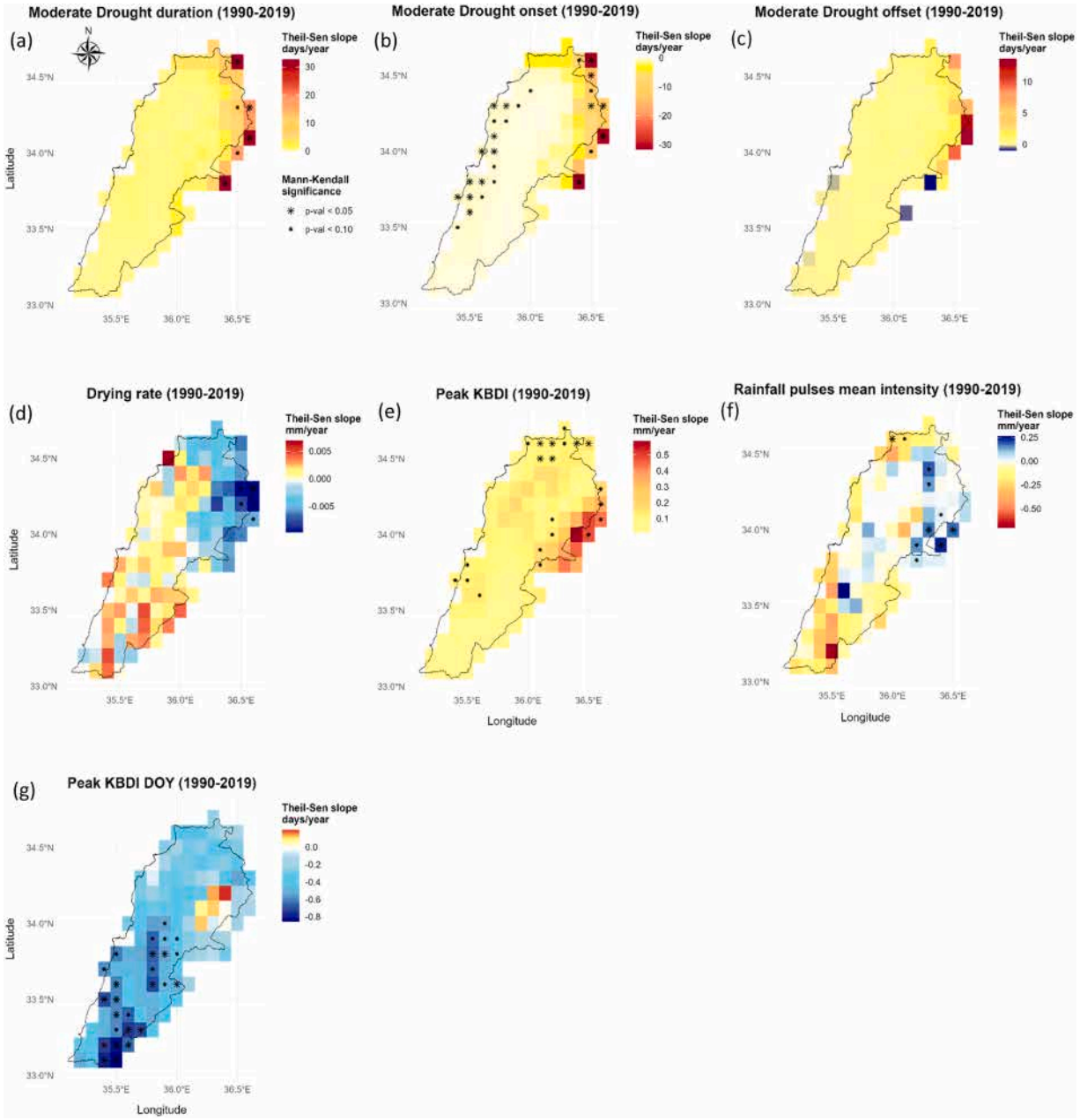

Fig. 8. Spatial distribution of Theil-Sen estimated slopes for the considered drought features (a-g) across Lebanon during the late period of 1990–2019. Smaller asterisks (*) indicate p-values less than 0.10, while larger asterisks (*) indicate p-values less than 0.05, as determined by the Mann-Kendall significance test. The absence of a symbol means that there is no statistically significant trend detected. Changes in drought conditions are directly reflected in the color gradient. A color gradient ranging from light yellow to dark red indicating an intensification of drought conditions (e.g., longer duration, earlier onset, delayed offset, higher peak severity, faster drying rate, and fewer rainfall pulses). In contrast, shades of blue indicate a decrease in drought conditions (e.g., shorter duration, delayed onset, earlier offset, lower peak severity, slower drying rate, and more rainfall pulses).

1990–2019 has become increasingly significant over the arid eastern regions of the country, rising by approximately + 7.5 mm (+0.25 mm/year) (Fig. 8f). However, a general decline is observed across the coastal and southern regions, with reductions ranging between −4.5 mm and −15 mm over the same timeframe.

4. Discussion

4.1. Temperature primarily drives regional drought dynamics beyond precipitation trends

Despite the absence of statistically significant precipitation trends over the past six decades in Lebanon (1960–2020), a reduction of approximately 70 mm over the wettest coastal areas out of an annual average of approximately 900 mm was observed. This decline is less pronounced in the already arid eastern regions of the country receiving as low as 250 mm of precipitation. In contrast, temperature trends exhibited a significant and consistent increase over the same period, ranging from approximately 0.7°C in the coastal areas to 1.2°C in the eastern regions. This continuous warming trend across the country, considering the average temperature differences among micro-climatic zones (i.e., 20°C over coastal areas, and 8°C over highest mountainous chains), is evident. It strongly suggests that rising temperatures are a primary driver of shifting and intensifying drought dynamics in Lebanon.

The observed warming trends are aligned with previous regional studies that have used either similar climatic datasets (i.e., ERA5-Land) or alternative sources such as ERA5 (Malik et al., 2024), CHELSA (Jaber et al., 2023), and daily station measurements which report a significant increase in mean temperatures across most of the eastern MB on the order of 0.1–0.6°C /decade (Almazroui, 2020; Donat et al., 2014; Jaber et al., 2023; Lionello and Scarascia, 2018; Malik et al., 2024; Zittis et al., 2022). Similar trends have also been documented for Lebanon, as highlighted by Verner et al. (2018). They reported an approximate increase by around 0.3°C/decade since 1970, based on observed annual mean air temperatures from two long-term recording stations in the country. Earlier studies by Ramadan et al., (2013a), (2013b), Shaban (2011), and Halwani and Halwani (2022) also documented comparable warming trends in Lebanon using a combination of global gridded datasets and local meteorological station data.

For precipitation, long-term trends remain less clear due to the complex interplay of large-scale climatic drivers, with the significance of trends varying notably between regions and studies across the MB (Ruffault et al., 2013; Zittis et al., 2022). Verner et al. (2018) noted that precipitation observations from two Lebanese stations (Beirut and Tripoli) were inconclusive in confirming an overall trend over the period 1900–2004. In contrast, Zittis (2018) reported a significant regional decrease in precipitation of approximately −8 mm/decade for 1901–2014, based on five gridded observational datasets. Similar findings have been observed for Lebanon by Ramadan et al., (2013a), (2013b) for the period 1900–2006. However, the finding of a non-significant 70 mm reduction over the past 60 years aligns with Shaban (2011), who reported a 50 mm decline in annual precipitation between 1960 and 2009, and with Kobrossi et al. (2021), who observed a reduction of −1.21 mm/year over the period 1926–2015 in Lebanon, all of which utilized a combination of climatic datasets (e.g., TRMM in order to fill the gaps in ground records) and local meteorological stations.

Yet, under these unsignificant precipitation trends and increasing temperatures, it is suggested by our findings that continuously rising temperatures play a crucial role in shaping regional drought trends in Lebanon (Liu et al., 2024b). Consistency with global and regional climate observations is also indicated, highlighting temperature-induced drought intensification. In these cases, higher evaporation rates and increased atmospheric moisture demand lead to earlier and prolonged drought events, even without significant changes in precipitation (Dai et al., 2022; Liu et al., 2023; Sheffield and Wood, 2008; Vicente-Serrano et al., 2022; Yuan et al., 2023). This underscores the importance of utilizing meaningful drought indices that incorporate key climatic factors, such as precipitation and air temperature, in drought trend assessments. Relying solely on precipitation statistics as a hallmark of climate change may overlook these critical national and regional drought dynamics (Elias et al., 2024; Ionita and Nagavciuc, 2021; Ruffault et al., 2013; Zellou et al., 2023).

4.2. Drought facets assessment detects earlier drought onset as a driver of prolonged duration

Over the past six decades (1960–2020), a slight and non-significant increase in drought duration across Lebanon is indicated by our results, aligning with observed precipitation patterns over the country. A deeper analysis of related drought features suggests that this prolonged duration is primarily driven by a significantly earlier drought onset, driven by continuous temperature increases. In contrast, drought duration appears to be less influenced by the timing of drought offset as evidenced by the absence of significant trends nationwide, albeit observed increased patterns.

The observed rises of drought durations, which follow a west-to-east gradient (15–135 days), align with previous assessments conducted across various Mediterranean regions which similarly reported an overall increasing trend in drought duration. For southern France, Ruffault et al. (2013) reported an increase in drought duration by around + 60 % to + 100 % estimated from daily soil water balance data over the period 1971–2006. Moreover, our observed increase in drought duration at a finer temporal resolution aligns broadly with the decadal analysis conducted by Ionita and Nagavciuc (2021) at the European level. Their study, based on SPI12 and SPEI12 for moderate drought level (between −1 and −1.5 as returned by the index), revealed a significant rise in the frequency of drought months per decade, increasing from approximately 20 months during 1951–1960–50 months in 2011–2019 across the region. Yet, despite our non-significant trend, Mathbout et al. (2018) identified a significant trend in Syria for the period 1961–2012. Their analysis was based on SPI and SPEI drought indices calculated from meteorological data obtained from 20 weather stations. Similarly, Páscoa et al. (2021) reported a significant trend in the Iberian Peninsula between 1971 and 2015 using a new gridded high-resolution dataset of daily precipitation and air temperatures (Iberia01).

It was observed that the significant shift toward earlier drought onset is a key contributor to the regional changes in increased drought duration. Several studies already reported this earlier drought onset in the MB over the las decades (Lempereur et al., 2017; Ruffault et al., 2013; Zribi et al., 2016) with earlier drought occurrences ranging from 5 to 80 days, which aligns with our findings under typical Mediterranean conditions where we observed a range of 7–17 days in the coastal areas. However, in certain very limited regions of our study area, especially the eastern most arid parts of the country, we recorded even greater earlier occurrences reaching

approximately 150 days, attributed to the frequent MYD events. Ultimately, it is demonstrated here that the DFEAT tool could serve as a promising resource for detecting historical trends of earlier drought onset occurrences, as well as for projecting future trends (Elias et al., 2024).

Over the past six decades, both drought duration and onset have shown clear patterns of intensification, with particularly pronounced changes during the sub-period 1990–2019. This shift marks a departure from the baseline conditions observed between 1960 and 1989 and indicates the onset of a regional drying trend beginning in the early 1990s, consistent with previous studies over the broader region (Cook et al., 2016; Mathbout et al., 2018; Ruffault et al., 2013). These increasing drought feature trends derived from DFEAT are consistent with recent findings for Lebanon based on conventional meteorological drought indices. In particular, Jomaa et al. (2024), using the SPI, reported a significant rise in drought severity since the 1990s. Although analyses based on SPI/SPEI offer less detailed insights compared to our feature-based approach, their results converge with ours. This agreement across independent approaches strengthens the evidence that Lebanon has experienced a marked intensification of drought conditions over the past three decades.

4.3. Drought features from DFEAT as hidden signals of recent climate change

In addition to addressing drought onset timing and associated duration, DFEAT enables a more nuanced assessment of specific drought features. These include drying rates, peak KBDI with its corresponding DOY, and rainfall pulse intensities, all of which are directly related to seasonal soil moisture depletion, propagation, and recovery. These features represent newly estimated climate change signals that have remained obscured in previous spatiotemporal trend analyses using standardized meteorological indices (Elias et al., 2024). Moreover, such finer drought signals are often difficult to detect through conventional temporal pattern analyses of precipitation and temperature (Kobrossi et al., 2021; Ramadan et al., 2013a, 2013b).

Recently, Yuan et al. (2023) demonstrated that earlier drought onset is strongly associated to accelerated soil moisture depletion on a global scale caused by an imbalance primarily driven by amplified anomalies in evapotranspiration and reductions in precipitation. Similarly, in China, Zhang et al. (2024) highlighted the rapid onset of drought as a consequence of the intricate interplay of these key climatic parameters. Drought onset assessment has recently garnered significant attention for its role in detecting the rapid development of drought. This rapid development is driven by the swift depletion of soil moisture, a phenomenon commonly referred in the literature as “flash droughts” (Christian et al., 2021; Ford et al., 2015; Yuan et al., 2023; Zeng et al., 2023). Our findings in this study corroborate this trend as demonstrated by an observed increase in soil moisture drying rates of + 0.0016 mm/year in the wettest areas of Mount Lebanon over the studied period 1960–2020. This suggests a combined influence of soil moisture depletion and atmospheric aridity in accelerating drying rates across some humid parts of the country (Qing et al., 2023, 2022). Further supporting the observed trend, the DFEAT sensitivity analyses performed by Elias et al. (2024) indicate that a 1°C to 2°C temperature rise amplifies drying rates by + 2 % to + 6 % compared to current conditions.

In parallel, the interplay between earlier drought onset and prolonged drought duration, driven by rising temperatures, exacerbates seasonal soil moisture deficit levels (or drought severity). Soils have more time to dry out between consecutive precipitation events (Mimeau et al., 2021; Nielsen et al., 2024). Higher evapotranspiration rates accelerate soil moisture loss through intensified soil evaporation and plant transpiration, beginning earlier in the season and further amplifying peak drought severity (Dai et al., 2022; Mondal et al., 2024; Zhang et al., 2025). This is particularly evident in the west-to-east gradient of peak drought severity trends which rises from 3 mm (out of an average of 190 mm) in the west to 15 mm (out of an average of 180 mm) in the east. Elias et al. (2024) identified a similar trend demonstrating that for every 1°C temperature increase drought severity intensifies by 10–15 %.

Simultaneously, regional declines in precipitation and its seasonal distribution limit water infiltration and hinder soil column replenishment, thereby extending the recovery period for soil moisture to compensate for seasonal deficits (McKellar and Crimmins, 2025; Nielsen et al., 2024; Yao et al., 2023). This is reflected in our study by the observed delayed drought offset trends and weakened intensities of autumn rainfall pulses. Regarding peak drought timing, our analysis reveals a non-significant shift toward earlier occurrences, ranging from 6 to 16 days across the country (out of an annual average around DOY 290), likely also primarily influenced by temperature rises pattern as previously noted by Elias et al. (2024). Their sensitivity analyses further emphasize this trend suggesting that for each degree of warming peak drought occurrence day advances by approximately + 2 % due to accelerated soil moisture depletion earlier in the season.

4.4. Implication of intensifying drought features on Lebanon’s agro-environmental systems

It has previously been demonstrated that a multifaceted approach encompassing seven key drought features offers deeper insights into recent and historical drought trends across spatial and temporal scales. Until now, these insights were buffered by the coarse monthly temporal resolution of standardized precipitation anomalies indices. This multifaceted consideration, which has revealed specific climate change impacts, should enable a more nuanced understanding of the national agro-environmental impacts. These includes areas burned by wildfires, rainfed crop yields, tree ring growth patterns, and other indicators associated with the intensification in particular drought features, as shown in Elias et al. (2025) for Lebanon. Recent years have witnessed growing interest in the compounding impact of drought features on agro-environmental threats. Researchers recognize that considering a wider range of drought features can exacerbate their overall impacts on the targeted variables. For instance, the duration and timing of drought have been strongly associated with the global decline in wheat crop yields when considered prior and during the growing season (Santini et al., 2022). Moreover, drought duration and severity over the months of June, July, and August have been closely correlated with the year-to-year variability in burned areas across the basin (Turco et al., 2017), with the particularity of drought offset driving burned

area in Lebanon (Elias et al., 2025; Majdalani et al., 2022). In forestry, drought duration, severity, and onset have also been found to significantly affect tree radial growth. These effects depends on which of the two non-mutually exclusive mechanisms occurs in response to drought: carbon starvation (or carbon assimilation) or limitation in growth phenology (related to cell turgor) (Cabon et al., 2024; Gao et al., 2018). Considering these mechanisms provides a more integrated index and a comprehensive understanding of related processes compared to the usual correlations between tree radial growth and time-lagged temperature or precipitation data (Zribi et al., 2016). Based on Elias et al. (2025) work on the relationships between drought features and agro-environmental threats in Lebanon, we suggest here that ongoing drought changes (earlier drought onset) might mostly affect wheat yields and tree growth. This is evidenced by a slow-down in wheat field productivity and frequent crop failures (http://faostat.fao.org/default.aspx), as well as reduced *Cedrus libani* productivity (Hajar et al., 2010). In contrast, burned area has not been significantly affected over the last decades (Majdalani et al., 2022).

4.5. Limitations and perspectives

We acknowledge the versatility of DFEAT as a novel tool capable of transforming daily soil moisture time series calculated using standard weather variables (air temperature and precipitation) into annual keystone drought features, simulated through the widely recognized KBDI index. Nevertheless, each drought index in the existing literature possesses its own advantages and limitations, shaped by the assumptions underlying its development and the specific climatic regions for which it was initially designed and applied (Zargar et al., 2011). For instance, the KBDI was originally developed for use in the United States (Keetch and Byram, 1968) and was later adapted and calibrated for use under Mediterranean conditions (Dimitrakopoulos and Bemmerzouk, 2003; Ganatsas et al., 2011; Garcia-Prats et al., 2015; Pellizzaro et al., 2007; Ruffault et al., 2018; Xanthopoulos et al., 2006).

As an initial application, DFEAT was standardized using the Mediterranean adapted KBDI version, adhering to its original assumptions with an empirical temperature-based equation for evapotranspiration calculation and a fixed field capacity of 200 mm (Elias et al., 2024; Ganatsas et al., 2011; Keetch and Byram, 1968). The generalization of this approach, however, may depend on site-specific factors such as soil texture and depth, which can be accounted for using available soil databases and maps(Ganatsas et al., 2011), although losing the genericity of the standard version. It is also important to acknowledge that the KBDI is an empirical rather than a physically based index, relying on simplified assumptions of soil water balance. As such, its performance can be sensitive to how drought thresholds are defined and is further limited by its lack of direct incorporation of key meteorological variables that strongly influence soil moisture, which may prevent it from consistently capturing soil–vegetation–atmosphere interactions across different ecosystems or climatic regimes. Ultimately, integrating an improved version of the KBDI index, incorporating refinements in the PET calculation using Priestley-Taylor or Penman-Monteith equation (McMahon et al., 2013), would account for essential parameters such as radiation and wind speed that could influence the soil moisture balance under climate change (Lemaitre-Basset et al., 2022). This would enable more accurate detection of annual drought features, which should be further evaluated.

Beyond KBDI, it is imperative to recognize that this tool's applicability extends to analogous daily simulated drought indices such as the Drought Code from the Canadian Fire Weather Index (Van Wagner, 1987). Its applicability extends to direct in-situ soil moisture measurements or process-based modeling of plant and soil water budget (Mouillot et al., 2001; Ruffault et al., 2013). In this regard, the DFEAT tool provides an efficient and robust alternative approach to conventional drought indices for detecting multifaceted drought features, along their trends and associated impacts (Elias et al., 2025). Its adaptability and reproducibility across diverse Mediterranean countries make it particularly valuable as it effectively functions across a spectrum of Mediterranean climates, from sub-humid to arid zones receiving as little as 200 mm of annual precipitation, as demonstrated in this study and prior works (Elias et al., 2024).

5. Conclusion

A comprehensive analysis of drought features in Lebanon, Middle-East, utilizing a multifaceted spatiotemporal approach through the DFEAT tool, reveals that a slight and statistically insignificant intensification of most features has been observed over the last six decades (1960–2020). This trend is primarily driven by a non-significant decline in annual rainfall but more particularly by a significant rise in air temperatures across the country. DFEAT appeared as an efficient tool to capture historical drought features trends monitoring as a response to climate change, and we strongly emphasize its potential usage as a critical tool for multifaceted drought trend analyses in Mediterranean climates. By considering multiple features of drought, DFEAT facilitates a more nuanced understanding of potential associated agro-environmental impacts, enabling the development of more targeted and effective mitigation strategies. Under recent and projected climatic conditions, the DFEAT tool enhances our ability to capture refined and subtle changes in specific drought features with finer temporal resolution, overcoming the limitations of traditional standardized indices constrained by coarser monthly scales. Such a spatiotemporal trend approach and the generated insights could inform water resource management and early warning systems, providing policymakers with updated, data-driven guidance to mitigate complex drought risks and plan adaptive strategies for vulnerable regions.

Funding

The project also received funding from the MENAFFIS specific action from IRD granted to Florent Mouilliot.

CRediT authorship contribution statement

ELIAS Georgie: Writing – original draft, Visualization, Software, Methodology, Formal analysis, Data curation, Conceptualization. **Georgia Majdalani:** Writing – review & editing, Visualization, Software, Methodology, Formal analysis. **Ghaleb Faour:** Writing – review & editing, Supervision, Resources, Funding acquisition, Conceptualization. **Florent Mouillot:** Writing – review & editing, Visualization, Validation, Supervision, Resources, Project administration, Methodology, Funding acquisition, Conceptualization.

Declaration of Competing Interest

The authors declare that they have no known competing financial interests or personal relationships that could have appeared to influence the work reported in this paper.

Acknowledgments

The authors acknowledge the National Council for Scientific Research of Lebanon (CNRS-L), the French Embassy in Lebanon, and Campus France for granting a doctoral fellowship to Georgie Elias (SAFAR program).

Appendix A. Supporting information

Supplementary data associated with this article can be found in the online version at doi:10.1016/j.ejrh.2025.102930.

Data availability

Data will be made available on request.

References

Aboelnour, M.A., Hamlet, A.F., Wood, D., Hung, F.-W., 2025. Leveraging ERA5-Land Reanalysis Precipitation Data for Urban Flood Vulnerability and Water Security Assessments: A Global Perspective. Earth Syst. Environ. 9, 2335–2353. https://doi.org/10.1007/s41748-025-00703-1.

Alexander, L.V., Zhang, X., Peterson, T.C., Caesar, J., Gleason, B., Klein Tank, A.M.G., Haylock, M., Collins, D., Trewin, B., Rahimzadeh, F., Tagipour, A., Rupa Kumar, K., Revadekar, J., Griffiths, G., Vincent, L., Stephenson, D.B., Burn, J., Aguilar, E., Brunet, M., Taylor, M., New, M., Zhai, P., Rusticucci, M., Vazquez-Aguirre, J.L., 2006. Global observed changes in daily climate extremes of temperature and precipitation. J. Geophys. Res. 111, 2005JD006290. https://doi.org/10.1029/2005JD006290.

Almazroui, M., 2020. Changes in Temperature Trends and Extremes over Saudi Arabia for the Period 1978–2019. Adv. Meteorol. 2020, 1–21. https://doi.org/10.1155/2020/8828421.

Al-Rimmawi, H., 2012. Middle East chronic water problems: solution prospects.

Amin, D., Keshta, E., Ragab, R., Chakrabortty, R., Elaksher, A.F., 2025. Impact of Climate Change on Hydrological Extremes (Floods and Droughts) in the Upper Blue Nile Basin. Earth Syst. Environ. https://doi.org/10.1007/s41748-025-00709-9.

Aschale, T.M., Cancelliere, A., Palazzolo, N., Buonacera, G., Peres, D.J., 2024. Analysis of the Spatiotemporal Trends of Standardized Drought Indices in Sicily Using ERA5-Land Reanalysis Data (1950–2023). Water 16, 2593. https://doi.org/10.3390/w16182593.

Azzopardi, B., Balzan, M.V., Cherif, S., Doblas-Miranda, E., dos Santos, M., Dobrinski, P., Falder, M., Hassoun, A.E.R., Giupponi, C., Koubi, V.V., 2020. Climate and environmental change in the Mediterranean basin–Current situation and risks for the future. First Mediterr. Assess. Rep.

Cabon, A., Ameztegui, A., Anderegg, W.R., Martínez-Vilalta, J., De Cáceres, M., 2024. Probing the interplay of biophysical constraints and photosynthesis to model tree growth. Agric. For. Meteorol. 345, 109852. https://doi.org/10.1016/j.agrformet.2023.109852.

Caloiero, T., Veltri, S., Caloiero, P., Frustaci, F., 2018. Drought analysis in Europe and in the Mediterranean basin using the standardized precipitation index. Water 10, 1043. https://doi.org/10.3390/w10081043.

Caloiero, T., Coscarelli, R., Gaudio, R., Leonardo, G.P., 2019. Precipitation trend and concentration in the Sardinia region. Theor. Appl. Clim. 137, 297–307. https://doi.org/10.1007/s00704-018-2595-1.

Camarero, J.J., Gazol, A., Sangüesa-Barreda, G., Oliva, J., Vicente-Serrano, S.M., 2015. To die or not to die: early warnings of tree dieback in response to a severe drought. J. Ecol. 103, 44–57. https://doi.org/10.1111/1365-2745.12295.

Carslaw, D.C., Ropkins, K., 2012. *openair* — An R package for air quality data analysis. Environ. Model. Softw. 2728 52–61. https://doi.org/10.1016/j.envsoft.2011.09.008.

Ceppi, A., Achite, M., Toubal, A.K., Caloiero, T., 2025. Mapping drought characteristics in northern Algerian Basins using the ERA5-Land dataset. Sci. Rep. 15, 10720. https://doi.org/10.1038/s41598-025-95418-8.

Choat, B., Brodribb, T.J., Brodersen, C.R., Duursma, R.A., López, R., Medlyn, B.E., 2018. Triggers of tree mortality under drought. Nature 558, 531–539. https://doi.org/10.1038/s41586-018-0240-x.

Christian, J.I., Basara, J.B., Hunt, E.D., Otkin, J.A., Furtado, J.C., Mishra, V., Xiao, X., Randall, R.M., 2021. Global distribution, trends, and drivers of flash drought occurrence. Nat. Commun. 12, 6330. https://doi.org/10.1038/s41467-021-26692-z.

Collins, M., Knutti, R., Arblaster, J., Dufresne, J.-L., Fichefet, T., Friedlingstein, P., Gao, X., Gutowski, W.J., Johns, T., Krinner, G., 2013. Long. Term. Clim. Chang. Proj. Commit. irreversibility.

Cook, B.I., Anchukaitis, K.J., Touchan, R., Meko, D.M., Cook, E.R., 2016. Spatiotemporal drought variability in the Mediterranean over the last 900 years. JGR Atmospheres 121, 2060–2074. https://doi.org/10.1002/2015JD023929.

Cos, J., Doblas-Reyes, F., Jury, M., Marcos, R., Bretonnière, P.-A., Samsó, M., 2022. The Mediterranean climate change hotspot in the CMIP5 and CMIP6 projections. Earth Syst. Dyn. 13, 321–340. https://doi.org/10.5194/esd-13-321-2022.

Coscarelli, R., Caloiero, T., Filice, E., Marsico, L., Rotundo, R., 2023. Meteorological Drought Characterization in the Calabria Region (Southern Italy). Climate 11, 160. https://doi.org/10.3390/cli11080160.

Crane, W.J.B., 1982. Computing grassland and forest fire behaviour, relative humidity and drought index by pocket calculator. Aust. For. 45, 89–97. https://doi.org/10.1080/00049158.1982.10674339.

Dai, A., 2013. Increasing drought under global warming in observations and models. Nat. Clim. Change 3, 52–58. https://doi.org/10.1038/NCLIMATE1633.
Dai, A., Trenberth, K.E., Qian, T., 2004. A global dataset of Palmer Drought Severity Index for 1870–2002: Relationship with soil moisture and effects of surface warming. J. Hydrometeorol. 5, 1117–1130. https://doi.org/10.1175/jhm-386.1.
Dai, X., Yu, Z., Matheny, A.M., Zhou, W., Xia, J., 2022. Increasing evapotranspiration decouples the positive correlation between vegetation cover and warming in the Tibetan plateau. Front. Plant Sci. 13. https://doi.org/10.3389/fpls.2022.974745.
Deng, S., Zhao, D., Chen, Z., Liu, L., Zhu, Y., Wang, K., Gao, X., Wu, H., Zheng, D., 2024. Global Distribution and Projected Variations of Compound Drought-Extreme Precipitation Events. e2024EF004809 Earth'S. Future 12. https://doi.org/10.1029/2024EF004809.
Deo, R.C., Byun, H.-R., Adamowski, J.F., Begum, K., 2017. Application of effective drought index for quantification of meteorological drought events: a case study in Australia. Theor. Appl. Clim. 128, 359–379. https://doi.org/10.1007/s00704-015-1706-5.
Dimitrakopoulos, A.P., Bemmerzouk, A.M., 2003. Predicting live herbaceous moisture content from a seasonal drought index. Int J. Biometeorol. 47, 73–79. https://doi.org/10.1007/s00484-002-0151-1.
Donat, M.G., Peterson, T.C., Brunet, M., King, A.D., Almazroui, M., Kolli, R.K., Boucherf, D., Al-Mulla, A.Y., Nour, A.Y., Aly, A.A., 2014. Changes in extreme temperature and precipitation in the Arab region: long-term trends and variability related to ENSO and NAO. Int. J. Climatol. 34. https://doi.org/10.1002/joc.3707.
Dong, Z., Liu, H., Baiyinbaoligao, Hu, H., Khan, M.Y.A., Wen, J., Chen, L., Tian, F., 2022. Future projection of seasonal drought characteristics using CMIP6 in the Lancang-Mekong River Basin. J. Hydrol. 610, 127815. https://doi.org/10.1016/j.jhydrol.2022.127815.
Dubrovský, M., Hayes, M., Duce, P., Trnka, M., Svoboda, M., Zara, P., 2014. Multi-GCM projections of future drought and climate variability indicators for the Mediterranean region. Reg. Environ. Change 14, 1907–1919. https://doi.org/10.1007/s10113-013-0562-z.
Elias, G., Faour, G., Mouillot, F., 2024. DFEAT: A multifaceted yearly Drought FEature Assessment Tool from daily soil water content. J. Hydrol., 131700 https://doi.org/10.1016/j.jhydrol.2024.131700.
Elias, G., Majdalani, G., Renard, D., Faour, G., Mouillot, F., 2025. Multiple asynchronous drought facets drive Mediterranean natural and cultivated ecosystems. Sci. Total Environ. 969, 178990. https://doi.org/10.1016/j.scitotenv.2025.178990.
Ernst, J., Stojanovic, M., Sorí, R., 2025. Long-term high-resolution multi-drought indices datasets for Austria derived from ERA5 Land Reanalysis. Data Brief. 61, 111807. https://doi.org/10.1016/j.dib.2025.111807.
Essa, Y.H., Hirschi, M., Thiery, W., El-Kenawy, A.M., Yang, C., 2023. Drought characteristics in Mediterranean under future climate change. npj Clim. Atmos. Sci. 6, 133. https://doi.org/10.1038/s41612-023-00458-4.
Felton, A.J., Knapp, A.K., Smith, M.D., 2021. Precipitation–productivity relationships and the duration of precipitation anomalies: An underappreciated dimension of climate change. Glob. Change Biol. 27, 1127–1140. https://doi.org/10.1111/gcb.15480.
Fick, S.E., Hijmans, R.J., 2017. WorldClim 2: new 1-km spatial resolution climate surfaces for global land areas. Int. J. Climatol. 37, 4302–4315. https://doi.org/10.1002/joc.5086.
Ford, T.W., McRoberts, D.B., Quiring, S.M., Hall, R.E., 2015. On the utility of in situ soil moisture observations for flash drought early warning in Oklahoma, USA. Geophys. Res. Lett. 42, 9790–9798. https://doi.org/10.1002/2015GL066600.
Fu, Z., Ciais, P., Wigneron, J.-P., Gentine, P., Feldman, A.F., Makowski, D., Viovy, N., Kemanian, A.R., Goll, D.S., Stoy, P.C., 2024. Global critical soil moisture thresholds of plant water stress. Nat. Commun. 15, 4826. https://doi.org/10.1038/s41467-024-49244-7.
Ganatsas, P., Antonis, M., Marianthi, T., 2011. Development of an adapted empirical drought index to the Mediterranean conditions for use in forestry. Agric. For. Meteor. 151, 241–250. https://doi.org/10.1016/j.agrformet.2010.10.011.
Gao, S., Liu, R., Zhou, T., Fang, W., Yi, C., Lu, R., Zhao, X., Luo, H., 2018. Dynamic responses of tree-ring growth to multiple dimensions of drought. Glob. Change Biol. 24, 5380–5390. https://doi.org/10.1111/gcb.14367.
Garcia-Prats, A., Tarcísio, F.J., Antonio, M.J., 2015. Development of a Keetch and Byram—Based drought index sensitive to forest management in Mediterranean conditions. Agric. For. Meteor. 205, 40–50. https://doi.org/10.1016/j.agrformet.2015.02.009.
Gatien, P., Arsenault, R., Martel, J.-L., St-Hilaire, A., 2023. Using the ERA5 and ERA5-Land reanalysis datasets for river water temperature modelling in a data-scarce region. Can. Water Resour. J. / Rev. Can. Des. Ressour. Hydr. 48, 93–110. https://doi.org/10.1080/07011784.2022.2113917.
Gherardi, L.A., Sala, O.E., 2015. Enhanced precipitation variability decreases grass- and increases shrub-productivity. Proc. Natl. Acad. Sci. U. S. A. 112, 12735–12740. https://doi.org/10.1073/pnas.1506433112.
Gomis-Cebolla, J., Rattayova, V., Salazar-Galán, S., Francés, F., 2023. Evaluation of ERA5 and ERA5-Land reanalysis precipitation datasets over Spain (1951–2020). Atmos. Res. 284, 106606. https://doi.org/10.1016/j.atmosres.2023.106606.
Gounmene, M., Guenang, G.M., Sonfack, B.R., Komkoua Mbienda, A.J., Sohtetcha Foking, R., Vondou, D.A., 2025. Spatiotemporal Trends in the Characteristics of Different Drought Categories in a Changing Climate Over Central-Africa. Earth Syst. Environ. https://doi.org/10.1007/s41748-025-00696-x.
Granier, A., Bréda, N., Biron, P., Villette, S., 1999. A lumped water balance model to evaluate duration and intensity of drought constraints in forest stands. Ecol. Model. 116, 269–283. https://doi.org/10.1016/S0304-3800(98)00205-1.
Gu, X., Li, J., Chen, Y.D., Kong, D., Liu, J., 2019. Consistency and Discrepancy of Global Surface Soil Moisture Changes From Multiple Model-Based Data Sets Against Satellite Observations. J. Geophys. Res. Atmospheres 124, 1474–1495. https://doi.org/10.1029/2018JD029304.
Hahn, C., Lüscher, A., Ernst-Hasler, S., Suter, M., Kahmen, A., 2021. Timing of drought in the growing season and strong legacy effects determine the annual productivity of temperate grasses in a changing climate. Biogeosciences 18, 585–604. https://doi.org/10.5194/bg-18-585-2021.
Hajar, L., François, L., Khater, C., Jomaa, I., Déqué, M., Cheddadi, R., 2010. Cedrus libani (A. Rich) distribution in Lebanon: Past, present and future. Comptes Rendus Biol. 333, 622–630. https://doi.org/10.1016/j.crvi.2010.05.003.
Halwani, J., Halwani, B., 2022. Climate Change in Lebanon and the Impact to Water Resources. In: Leal Filho, W., Manolas, E. (Eds.), Climate Change in the Mediterranean and Middle Eastern Region, Climate Change Management. Springer International Publishing, Cham, pp. 395–412. https://doi.org/10.1007/978-3-030-78566-6_19.
Hamadeh, N., Karouni, A., Daya, B., Chauvet, P., 2017. Using correlative data analysis to develop weather index that estimates the risk of forest fires in Lebanon & Mediterranean: Assessment versus prevalent meteorological indices. Case Stud. Fire Saf. 7, 8–22. https://doi.org/10.1016/j.csfs.2016.12.001.
Häusler, M., Nunes, J.P., Silva, J.M., Keizer, J.J., Warneke, T., Pereira, J.M., 2019. A promising new approach to estimate drought indices for fire danger assessment using remotely sensed data. Agric. For. Meteor. 274, 195–209. https://doi.org/10.1016/j.agrformet.2019.04.015.
Hertig, E., Tramblay, Y., 2017. Regional downscaling of Mediterranean droughts under past and future climatic conditions. Glob. Planet. Change 151, 36–48. https://doi.org/10.1016/j.gloplacha.2016.10.015.
Ionita, M., Nagavciuc, V., 2021. Changes in drought features at the European level over the last 120 years. Nat. Hazards Earth Syst. Sci. 21, 1685–1701. https://doi.org/10.5194/nhess-21-1685-2021.
Jaber, S.M., Abu-Allaban, M.M., Sengupta, R., 2023. Spatial and temporal patterns of indicators of climate change and variability in the Arab world in the past four decades. Sci. Rep. 13, 15145. https://doi.org/10.1038/s41598-023-42499-y.
Jeong, M.-S., Park, S.-Y., Kim, Y.-J., Yoon, H.-C., Lee, J.-H., 2024. Identification of propagation characteristics from meteorological drought to hydrological drought using daily drought indices and lagged correlations analysis. J. Hydrol. Reg. Stud. 55, 101939. https://doi.org/10.1016/j.ejrh.2024.101939.
Jomaa, I., Abi Saab, M.T., Skaf, S., El Haj, N., Massaad, R., 2019. Variability in spatial distribution of precipitation overall rugged topography of Lebanon, using TRMM images. Atmos. Clim. Sci. 9 369–380. https://doi.org/10.4236/acs.2019.93026.
Jomaa, I., Choker, M., Haj, N.E., Saab, M.T.A., Funaro, M., Mereu, S., 2024. Levant Drought Occurrence, Lebanon Case. Atmos. Clim. Sci. 14, 118–127. https://doi.org/10.4236/acs.2024.141007.
Karger, D.N., Conrad, O., Böhner, J., Kawohl, T., Kreft, H., Soria-Auza, R.W., Zimmermann, N.E., Linder, H.P., Kessler, M., 2017. Climatologies at high resolution for the earth's land surface areas. Sci. Data 4, 170122. https://doi.org/10.1038/sdata.2017.122.
Keeley, J.E., Brennan, T.J., Syphard, A.D., 2022. The effects of prolonged drought on vegetation dieback and megafires in southern California chaparral. Ecosphere 13, e4203. https://doi.org/10.1002/ecs2.4203.

Keetch, J.J., Byram, G.M., 1968. A drought index for forest fire control. Southeastern Forest Experiment. US Department of Agriculture, Forest Service.
Kendall, M.G., 1975. Rank correlation methods. Griffin, London. J. Econom 13, 245–259.
Kesgin, E., Yaldız, S.G., Güçlü, Y.S., 2024. Spatiotemporal variability and trends of droughts in the Mediterranean coastal region of Türkiye. Int. J. Climatol. 44, 1036–1057. https://doi.org/10.1002/joc.8370.
Keune, J., Di Giuseppe, F., Barnard, C., Damasio da Costa, E., Wetterhall, F., 2025. ERA5–Drought: Global drought indices based on ECMWF reanalysis. Sci. Data 12, 616. https://doi.org/10.1038/s41597-025-04896-y.
Kim, D.-W., Byun, H.-R., Choi, K.-S., 2009. Evaluation, modification, and application of the effective drought index to 200-year drought climatology of Seoul, Korea. J. Hydrol. 378, 1–12. https://doi.org/10.1016/j.jhydrol.2009.08.021.
Klein, T., 2014. The variability of stomatal sensitivity to leaf water potential across tree species indicates a continuum between isohydric and anisohydric behaviours. Funct. Ecol. 28, 1313–1320. https://doi.org/10.1111/1365-2435.12289.
Kobrossi, J., Karam, F., Mitri, G., 2021. Rain pattern analysis using the Standardized Precipitation Index for long-term drought characterization in Lebanon. Arab. J. Geosci. 14, 1–17. https://doi.org/10.1007/s12517-020-06387-3.
Koutroulis, A.G., Vrohidou, A.-E.K., Tsanis, I.K., 2011. Spatiotemporal characteristics of meteorological drought for the island of Crete. J. Hydrometeorol. 12, 206–226. https://doi.org/10.1175/2010JHM1252.1.
Koutsias, N., Xanthopoulos, G., Founda, D., Xystrakis, F., Nioti, F., Pleniou, M., Mallinis, G., Arianoutsou, M., 2012. On the relationships between forest fires and weather conditions in Greece from long-term national observations (1894–2010). Int. J. Wildland Fire 22, 493–507. https://doi.org/10.1071/WF12003.
Lemaitre-Basset, T., Oudin, L., Thirel, G., Collet, L., 2022. Unraveling the contribution of potential evaporation formulation to uncertainty under climate change. Hydrol. Earth Syst. Sci. 26, 2147–2159. https://doi.org/10.5194/hess-26-2147-2022.
Lempereur, M., Martin-StPaul, N.K., Damesin, C., Joffre, R., Ourcival, J., Rocheteau, A., Rambal, S., 2015. Growth duration is a better predictor of stem increment than carbon supply in a M editerranean oak forest: implications for assessing forest productivity under climate change. N. Phytol. 207, 579–590. https://doi.org/10.1111/nph.13400.
Lempereur, M., Limousin, J., Guibal, F., Ourcival, J., Rambal, S., Ruffault, J., Mouillot, F., 2017. Recent climate hiatus revealed dual control by temperature and drought on the stem growth of Mediterranean *Quercus ilex*. Glob. Change Biol. 23, 42–55. https://doi.org/10.1111/gcb.13495.
Li, X., Zhang, G., Zhu, S., Xu, Y., 2025. Stepwise Downscaling of ERA5-Land Reanalysis Air Temperature: A Case Study in Nanjing, China. Remote Sens. 17, 2063. https://doi.org/10.3390/rs17122063.
Lionello, P., Scarascia, L., 2018. The relation between climate change in the Mediterranean region and global warming. Reg. Environ. Change 18, 1481–1493. https://doi.org/10.1007/s10113-018-1290-1.
Liu, J., Ma, X., Duan, Z., Jiang, J., Reichstein, M., Jung, M., 2020. Impact of temporal precipitation variability on ecosystem productivity. WIREs Water 7, e1481. https://doi.org/10.1002/wat2.1481.
Liu, Y., Wang, Z., Zhang, X., Zhu, Y., Ren, L., Yuan, S., Jin, J., 2024b. Accelerated soil moisture drought onset link to high temperatures and asymmetric responses associated with the hit timing. Hydrol. Earth Syst. Sci. Discuss. 1–19. https://doi.org/10.5194/hess-2024-199.
Liu, Y., Yang, Y., Song, J., 2023. Variations in Global Soil Moisture During the Past Decades: Climate or Human Causes? Water Resour. Res. 59, e2023WR034915. https://doi.org/10.1029/2023WR034915.
Liu, H., Wang, X., Liang, C., Xue, P., Wang, Z., Chen, Y., Zhang, M., 2024a. Divergent nonlinear trends of global drought and its multivariate characteristics. J. Hydrol. 630, 130759. https://doi.org/10.1016/j.jhydrol.2024.130759.
Majdalani, G., Koutsias, N., Faour, G., Adjizian-Gerard, J., Mouillot, F., 2022. Fire Regime Analysis in Lebanon (2001–2020): Combining Remote Sensing Data in a Scarcely Documented Area. Fire 5, 141. https://doi.org/10.3390/fire5050141.
Malik, A., Stenchikov, G., Mostamandi, S., Parajuli, S., Lelieveld, J., Zittis, G., Ahsan, M.S., Atique, L., Usman, M., 2024. Accelerated Historical and Future Warming in the Middle East and North Africa. JGR Atmospheres 129, e2024JD041625. https://doi.org/10.1029/2024JD041625.
Mann, H.B., 1945. Nonparametric tests against trend. Économ. J. Econom. Soc. 245–259.
Marcos-Garcia, P., Lopez-Nicolas, A., Pulido-Velazquez, M., 2017. Combined use of relative drought indices to analyze climate change impact on meteorological and hydrological droughts in a Mediterranean basin. J. Hydrol. 554, 292–305. https://doi.org/10.1016/j.jhydrol.2017.09.028.
Martins Careto, J.A., Cardoso, R.M., Russo, A., André Lima, D.C., Matos Soares, P.M., 2024. Generalised drought index: a novel multi-scale daily approach for drought assessment. Geosci. Model Dev. 17, 8115–8139. https://doi.org/10.5194/gmd-17-8115-2024.
Mathbout, S., Lopez-Bustins, J.A., Martin-Vide, J., Bech, J., Rodrigo, F.S., 2018. Spatial and temporal analysis of drought variability at several time scales in Syria during 1961–2012. Atmos. Res. 200, 153–168. https://doi.org/10.1016/j.atmosres.2017.09.016.
Mathbout, S., Lopez-Bustins, J.A., Royé, D., Martin-Vide, J., 2021. Mediterranean-scale drought: Regional datasets for exceptional meteorological drought events during 1975–2019. Atmosphere 12, 941. https://doi.org/10.3390/atmos12080941.
Mathbout, S., Martin-Vide, J., Bustins, J.A.L., 2023. Drought characteristics projections based on CMIP6 climate change scenarios in Syria. J. Hydrol. Reg. Stud. 50, 101581. https://doi.org/10.1016/j.ejrh.2023.101581.
McKee, T.B., Doesken, N.J., Kleist, J., 1993. The relationship of drought frequency and duration to time scales, in: Proceedings of the 8th Conference on Applied Climatology. California, pp. 179–183.
McKellar, T.T., Crimmins, M.A., 2025. Seasonal precipitation variability controls shallow soil water drought events across the southwestern United States. Agric. For. Meteorol. 363, 110403. https://doi.org/10.1016/j.agrformet.2025.110403.
McLeod, A.I., 2005. Kendall rank correlation and Mann-Kendall trend test. R. Package Kendall 602, 1–10.
McMahon, T.A., Peel, M.C., Lowe, L., Srikanthan, R., McVicar, T.R., 2013. Estimating actual, potential, reference crop and pan evaporation using standard meteorological data: a pragmatic synthesis. Hydrol. Earth Syst. Sci. 17, 1331–1363. https://doi.org/10.5194/hess-17-1331-2013.
Mfarrej, M.F.B., 2025. Exploring the nexus between climate change, water scarcity, and security dynamics in the Middle East and North Africa. Research 2, 100168. https://doi.org/10.1016/j.nexres.2025.100168.
Mimeau, L., Tramblay, Y., Brocca, L., Massari, C., Camici, S., Finaud-Guyot, P., 2021. Modeling the response of soil moisture to climate variability in the Mediterranean region. Hydrol. Earth Syst. Sci. 25, 653–669. https://doi.org/10.5194/hess-25-653-2021.
Minea, I., Albulescu, A.-C., 2025. Drought Over Time: an Investigation of the Impact of Meteorological Drought on Groundwater and Surface Water in the East of Romania. Earth Syst. Environ. 9, 1959–1981. https://doi.org/10.1007/s41748-025-00725-9.
Mishra, A.K., Singh, V.P., 2010. A review of drought concepts. J. Hydrol. 391, 202–216. https://doi.org/10.1016/j.jhydrol.2010.07.012.
Mitri, G., Jazi, M., McWethy, D., 2014. Investigating temporal and spatial variability of wildfire potential with the use of objectbased image analysis of downscaled global climate models. SouthEast. Eur. J. Earth Obs. Geomat. 3, 251–254.
Miyan, M.A., 2015. Droughts in Asian Least Developed Countries: Vulnerability and sustainability. In: Weather and Climate Extremes, 7. SI: IGBP APN, pp. 8–23. https://doi.org/10.1016/j.wace.2014.06.003.
Mondal, S.K., An, S.-I., Min, S.-K., Jiang, T., Su, B., 2024. Enhanced soil moisture–temperature coupling could exacerbate drought under net-negative emissions. npj Clim. Atmos. Sci. 7, 1–12. https://doi.org/10.1038/s41612-024-00820-0.
Mouillot, F., Rambal, S., Lavorel, S., 2001. A generic process-based SImulator for meditERRanean landscApes (SIERRA): design and validation exercises. For. Ecol. Manag. 147, 75–97. https://doi.org/10.1016/S0378-1127(00)00432-1.
Muñoz-Sabater, J., Dutra, E., Agustí-Panareda, A., Albergel, C., Arduini, G., Balsamo, G., Boussetta, S., Choulga, M., Harrigan, S., Hersbach, H., 2021. ERA5-Land: A state-of-the-art global reanalysis dataset for land applications. Earth Syst. Sci. data 13, 4349–4383. https://doi.org/10.5194/essd-13-4349-2021.
Nielsen, M., Cook, B.I., Marvel, K., Ting, M., Smerdon, J.E., 2024. The Changing Influence of Precipitation on Soil Moisture Drought With Warming in the Mediterranean and Western North America. Earth'S. Future 12, e2023EF003987. https://doi.org/10.1029/2023EF003987.
Onyutha, C., 2017. On rigorous drought assessment using daily time scale: Non-stationary frequency analyses, revisited concepts, and a new method to yield non-parametric indices. Hydrology 4, 48. https://doi.org/10.3390/hydrology4040048.

Páscoa, P., Gouveia, C.M., Russo, A., Trigo, R.M., 2017. The role of drought on wheat yield interannual variability in the Iberian Peninsula from 1929 to 2012. Int. J. Biometeorol. 61, 439–451. https://doi.org/10.1007/s00484-016-1224-x.
Páscoa, P., Russo, A., Gouveia, C.M., Soares, P.M.M., Cardoso, R.M., Careto, J.A.M., Ribeiro, A.F.S., 2021. A high-resolution view of the recent drought trends over the Iberian Peninsula. Weather Clim. Extrem. 32, 100320. https://doi.org/10.1016/j.wace.2021.100320.
Pellizzaro, G., Cesaraccio, C., Duce, P., Ventura, A., Zara, P., 2007. Relationships between seasonal patterns of live fuel moisture and meteorological drought indices for Mediterranean shrubland species. Int. J. Wildland Fire 16, 232–241. https://doi.org/10.1071/WF06081.
Politi, N., Vlachogiannis, D., Sfetsos, A., Nastos, P.T., Dalezios, N.R., 2022. High resolution future projections of drought characteristics in Greece based on SPI and SPEI indices. Atmosphere 13, 1468. https://doi.org/10.3390/atmos13091468.
Qing, Y., Wang, S., Ancell, B.C., Yang, Z.-L., 2022. Accelerating flash droughts induced by the joint influence of soil moisture depletion and atmospheric aridity. Nat. Commun. 13, 1139. https://doi.org/10.1038/s41467-022-28752-4.
Qing, Y., Wang, S., Yang, Z.-L., Gentine, P., Zhang, B., Alexander, J., 2023. Accelerated soil drying linked to increasing evaporative demand in wet regions. npj Clim. Atmos. Sci. 6, 205. https://doi.org/10.1038/s41612-023-00531-y.
Ramadan, H.H., Beighley, R.E., Ramamurthy, A.S., 2013a. Temperature and Precipitation Trends in Lebanon's Largest River: The Litani Basin. J. Water Resour. Plann. Manag. 139, 86–95. https://doi.org/10.1061/(ASCE)WR.1943-5452.0000238.
Ramadan, H.H., Beighley, R.E., Ramamurthy, A.S., 2013b. Temperature and Precipitation Trends in Lebanon's Largest River: The Litani Basin. J. Water Resour. Plan. Manag. 139, 86–95. https://doi.org/10.1061/(ASCE)WR.1943-5452.0000238.
Rambal, S., Lempereur, M., Limousin, J.-M., Martin-StPaul, N.K., Ourcival, J.-M., Rodriguez-Calcerrada, J., 2014. How drought severity constrains gross primary production (GPP) and its partitioning among carbon pools in a Quercus ilex coppice? Biogeosciences 11, 6855–6869. https://doi.org/10.5194/bg-11-6855-2014.
Řehoř, J., Trnka, M., Brázdil, R., Fischer, M., Balek, J., van der Schrier, G., Feng, S., 2023. Global hotspots in soil moisture-based drought trends. Environ. Res. Lett. 19, 014021. https://doi.org/10.1088/1748-9326/ad0f01.
Reinecke, R., Müller Schmied, H., Trautmann, T., Andersen, L.S., Burek, P., Flörke, M., Gosling, S.N., Grillakis, M., Hanasaki, N., Koutroulis, A., 2021. Uncertainty of simulated groundwater recharge at different global warming levels: a global-scale multi-model ensemble study. Hydrol. Earth Syst. Sci. 25, 787–810. https://doi.org/10.5194/hess-25-787-2021.
Ribeiro, A.F.S., Russo, A., Gouveia, C.M., Páscoa, P., 2019. Modelling drought-related yield losses in Iberia using remote sensing and multiscalar indices. Theor. Appl. Clim. 136, 203–220. https://doi.org/10.1007/s00704-018-2478-5.
Richardson, D., Black, A.S., Irving, D., Matear, R.J., Monselesan, D.P., Risbey, J.S., Squire, D.T., Tozer, C.R., 2022. Global increase in wildfire potential from compound fire weather and drought. NPJ Clim. Atmos. Sci. 5, 23. https://doi.org/10.1038/s41612-022-00248-4.
Ritter, F., Berkelhammer, M., Garcia, C., 2020. Distinct response of gross primary productivity in five terrestrial biomes to precipitation variability. Commun. Earth Environ. 1, 34. https://doi.org/10.1038/s43247-020-00034-1.
Ruffault, J., Martin-StPaul, N.K., Rambal, S., Mouillot, F., 2013. Differential regional responses in drought length, intensity and timing to recent climate changes in a Mediterranean forested ecosystem. Clim. Chang 117, 103–117 https://doi.org/0.1007/s10584-012-0559-5.
Ruffault, J., Martin-StPaul, N., Pimont, F., Dupuy, J.-L., 2018. How well do meteorological drought indices predict live fuel moisture content (LFMC)? An assessment for wildfire research and operations in Mediterranean ecosystems. Agric. For. Meteor. 262, 391–401. https://doi.org/10.1016/j.agrformet.2018.07.031.
Ruffault, J., Limousin, J., Pimont, F., Dupuy, J., De Càceres, M., Cochard, H., Mouillot, F., Blackman, C.J., Torres-Ruiz, J.M., Parsons, R.A., Moreno, M., Delzon, S., Jansen, S., Olioso, A., Choat, B., Martin-StPaul, N., 2023. Plant hydraulic modelling of leaf and canopy fuel moisture content reveals increasing vulnerability of a Mediterranean forest to wildfires under extreme drought. N. Phytol. 237, 1256–1269. https://doi.org/10.1111/nph.18614.
Russo, A., Gouveia, C.M., Páscoa, P., DaCamara, C.C., Sousa, P.M., Trigo, R.M., 2017. Assessing the role of drought events on wildfires in the Iberian Peninsula. Agric. For. Meteorol. 237, 50–59. https://doi.org/10.1016/j.agrformet.2017.01.021.
Sakellariou, S., Dalezios, N.R., Spiliotopoulos, M., Alpanakis, N., Faraslis, I., Tziatzios, G.A., Sidiropoulos, P., Dercas, N., Domínguez, A., López, H.M., 2024. Remotely Sensed Comparative Spatiotemporal Analysis of Drought and Wet Periods in Distinct Mediterranean Agroecosystems. Remote Sens. 16, 3652. https://doi.org/10.3390/rs16193652.
Salesa, D., Baeza, M.J., Santana, V.M., 2024. Fire severity and prolonged drought do not interact to reduce plant regeneration capacity but alter community composition in a Mediterranean shrubland. fire Ecol. 20, 61. https://doi.org/10.1186/s42408-024-00292-w.
Santini, M., Noce, S., Antonelli, M., Caporaso, L., 2022. Complex drought patterns robustly explain global yield loss for major crops. Sci. Rep. 12, 5792. https://doi.org/10.1038/s41598-022-09611-0.
Saxton, K.E., Rawls, W.J., 2006. Soil Water Characteristic Estimates by Texture and Organic Matter for Hydrologic Solutions. Soil Sci. Soc. Am. J. 70, 1569–1578. https://doi.org/10.2136/sssaj2005.0117.
Sen, P.K., 1968. Estimates of the Regression Coefficient Based on Kendall's Tau. J. Am. Stat. Assoc. 63, 1379–1389. https://doi.org/10.1080/01621459.1968.10480934.
Shaban, A., 2011. Analyzing climatic and hydrologic trends in Lebanon. J. Environ. Sci. Eng. 5.
Shaban, A., 2020. Water Resources of Lebanon. World Water Resources. Springer International Publishing, Cham. https://doi.org/10.1007/978-3-030-48717-1.
Shaban, A., Houhou, R., 2015. Drought or humidity oscillations? The case of coastal zone of Lebanon. J. Hydrol. 529, 1768–1775. https://doi.org/10.1016/j.jhydrol.2015.08.010.
Shaban, A., Awad, M., Ghandour, A.J., Telesca, L., 2019. A 32-year aridity analysis: a tool for better understanding on water resources management in Lebanon. Acta Geophys 67, 1179–1189. https://doi.org/10.1007/s11600-019-00300-7.
Sheffield, J., Wood, E.F., 2008. Global trends and variability in soil moisture and drought characteristics, 1950–2000, from observation-driven simulations of the terrestrial hydrologic cycle. J. Clim. 21, 432–458. https://doi.org/10.1175/2007JCLI1822.1.
Slette, I.J., Post, A.K., Awad, M., Even, T., Punzalan, A., Williams, S., Smith, M.D., Knapp, A.K., 2019. How ecologists define drought, and why we should do better. Glob. Change Biol. 25, 3193–3200. https://doi.org/10.1111/gcb.14747.
Sousa, P.M., Trigo, R.M., Aizpurua, P., Nieto, R., Gimeno, L., Garcia-Herrera, R., 2011. Trends and extremes of drought indices throughout the 20th century in the Mediterranean. Nat. Hazards Earth Syst. Sci. 11, 33–51. https://doi.org/10.5194/nhess-11-33-2011.
Tramblay, Y., Koutroulis, A., Samaniego, L., Vicente-Serrano, S.M., Volaire, F., Boone, A., Le Page, M., Llasat, M.C., Albergel, C., Burak, S., 2020. Challenges for drought assessment in the Mediterranean region under future climate scenarios. EarthSci. Rev. 210, 103348.
Tsesmelis, D.E., Leveidioti, I., Karavitis, C.A., Kalogeropoulos, K., Vasilakou, C.G., Tsatsaris, A., Zervas, E., 2023. Spatiotemporal application of the standardized precipitation index (SPI) in the eastern Mediterranean. Climate 11, 95. https://doi.org/10.3390/cli11050095.
Tuel, A., Eltahir, E.A., 2020. Why is the Mediterranean a climate change hot spot? J. Clim. 33, 5829–5843. https://doi.org/10.1175/JCLI-D-19-0910.1.
Turco, M., von Hardenberg, J., AghaKouchak, A., Llasat, M.C., Provenzale, A., Trigo, R.M., 2017. On the key role of droughts in the dynamics of summer fires in Mediterranean Europe. Sci. Rep. 7, 81. https://doi.org/10.1038/s41598-017-00116-9.
Ullah, W., Alabduoli, K., Ullah, S., Al-Ghamdi, S.G., Alhebsi, K., Almazroui, M., Assiri, M.E., Azeem, W., Abuelgasim, A., Hagan, D.F.T., 2024. Comparison of 2-m surface temperature data between reanalysis and observations over the Arabian Peninsula. Atmos. Res. 311, 107725. https://doi.org/10.1016/j.atmosres.2024.107725.
Valeriano, C., Gazol, A., Colangelo, M., Camarero, J.J., 2021. Drought drives growth and mortality rates in three pine species under Mediterranean conditions. Forests 12, 1700. https://doi.org/10.3390/f12121700.
Van Wagner, C.E., 1987. Development and structure of the Canadian forest fire weather index system.
Verner, D., Ashwill, M., Christensen, J., Mcdonnell, R., Redwood, J., Jomaa, I., Saade, M., Massad, R., Chehade, A., Bitar, A., 2018. Droughts Agric. Leban.
Vicente-Serrano, S.M., Beguería, S., López-Moreno, J.I., 2010. A multiscalar drought index sensitive to global warming: the standardized precipitation evapotranspiration index. J. Clim. 23, 1696–1718. https://doi.org/10.1175/2009JCLI2909.1.
Vicente-Serrano, S.M., Lopez-Moreno, J.-I., Beguería, S., Lorenzo-Lacruz, J., Sanchez-Lorenzo, A., García-Ruiz, J.M., Azorin-Molina, C., Morán-Tejeda, E., Revuelto, J., Trigo, R., 2014. Evidence of increasing drought severity caused by temperature rise in southern Europe. Environ. Res. Lett. 9, 044001.

Vicente-Serrano, S.M., Peña-Angulo, D., Beguería, S., Domínguez-Castro, F., Tomás-Burguera, M., Noguera, I., Gimeno-Sotelo, L., El Kenawy, A., 2022. Global drought trends and future projections. Philos. Trans. R. Soc. A. 380, 20210285. https://doi.org/10.1098/rsta.2021.0285.

Waha, K., Krummenauer, L., Adams, S., Aich, V., Baarsch, F., Coumou, D., Fader, M., Hoff, H., Jobbins, G., Marcus, R., Mengel, M., Otto, I.M., Perrette, M., Rocha, M., Robinson, A., Schleussner, C.-F., 2017. Climate change impacts in the Middle East and Northern Africa (MENA) region and their implications for vulnerable population groups. Reg. Environ. Change 17, 1623–1638. https://doi.org/10.1007/s10113-017-1144-2.

Walker, D.W., Van Loon, A.F., 2023. Droughts are coming on faster. Science 380, 130–132. https://doi.org/10.1126/science.adh3097.

Wang, S.-P., Zhang, Q., Liu, Y.-Z., Yue, P., Wang, J.-S., 2024. Effects of global warming on drought onset in China. J. Hydrol. 632, 130964. https://doi.org/10.1016/j.jhydrol.2024.130964.

Wilhite, D.A., 2016. Drought as a natural hazard: concepts and definitions. in: Droughts. Routledge, pp. 3–18.

Wilhite, D.A., Glantz, M.H., 1985. Understanding: the Drought Phenomenon: The Role of Definitions. Water Int. 10, 111–120. https://doi.org/10.1080/02508068508686328.

Xanthopoulos, G., Maheras, G., Gouma, V., Gouvas, M., 2006. Is the Keetch-Byram drought index (KBDI) directly related to plant water stress? For. Ecol. Manag 234, S27. https://doi.org/10.1016/j.foreco.2006.08.043.

Xu, L., Wang, A., Wang, D., Wang, H., 2019. Hot Spots of Climate Extremes in the Future. JGR Atmospheres 124, 3035–3049. https://doi.org/10.1029/2018JD029980.

Yao, Y., Liu, Y., Zhou, S., Song, J., Fu, B., 2023. Soil moisture determines the recovery time of ecosystems from drought. Glob. Change Biol. 29, 3562–3574. https://doi.org/10.1111/gcb.16620.

Yihdego, Y., Vaheddoost, B., Al-Weshah, R.A., 2019. Drought indices and indicators revisited. Arab J. Geosci. 12, 69. https://doi.org/10.1007/s12517-019-4237-z.

Yuan, X., Wang, Y., Ji, P., Wu, P., Sheffield, J., Otkin, J.A., 2023. A global transition to flash droughts under climate change. Science 380, 187–191. https://doi.org/10.1126/science.abn6301.

Zargar, A., Sadiq, R., Naser, B., Khan, F.I., 2011. A review of drought indices. Environ. Rev. 19, 333–349. https://doi.org/10.1139/a11-013.

Zellou, B., El Moçayd, N., Bergou, E.H., 2023. Review article: Towards improved drought prediction in the Mediterranean region – modeling approaches and future directions. Nat. Hazards Earth Syst. Sci. 23, 3543–3583. https://doi.org/10.5194/nhess-23-3543-2023.

Zeng, Z., Wu, W., Peñuelas, J., Li, Y., Jiao, W., Li, Z., Ren, X., Wang, K., Ge, Q., 2023. Increased risk of flash droughts with raised concurrent hot and dry extremes under global warming. npj Clim. Atmos. Sci. 6, 134. https://doi.org/10.1038/s41612-023-00468-2.

Zhang, J., Zhang, M., Yu, J., Yu, Y., Jiang, F., Yu, R., 2024. Identifying and characterizing short-term drought with rapid onset based on the SAPEI in the Yangtze River basin. J. Hydrol. Reg. Stud. 51, 101629. https://doi.org/10.1016/j.ejrh.2023.101629.

Zhang, W., Furtado, K., Wu, P., Zhou, T., Chadwick, R., Marzin, C., Rostron, J., Sexton, D., 2021. Increasing precipitation variability on daily-to-multiyear time scales in a warmer world. Sci. Adv. 7, eabf8021. https://doi.org/10.1126/sciadv.abf8021.

Zhang, X., Wang, X., Zohner, C.M., Peñuelas, J., Li, Y., Wu, X., Zhang, Y., Liu, H., Shen, P., Jia, X., Liu, W., Tian, D., Pradhan, P., Fandohan, A.B., Peng, D., Wu, C., 2025. Declining precipitation frequency may drive earlier leaf senescence by intensifying drought stress and enhancing drought acclimation. Nat. Commun. 16, 910. https://doi.org/10.1038/s41467-025-56159-4.

Zhang, Y., Li, J., Liu, D., 2024. Spatial Downscaling of ERA5 Reanalysis Air Temperature Data Based on Stacking Ensemble Learning. Sustainability 16, 1934. https://doi.org/10.3390/su16051934.

Zhu, Z., Duan, W., Zou, S., Zeng, Z., Chen, Y., Feng, M., Qin, J., Liu, Y., 2024. Spatiotemporal characteristics of meteorological drought events in 34 major global river basins during 1901–2021. Sci. Total Environ. 921, 170913. https://doi.org/10.1016/j.scitotenv.2024.170913.

Zittis, G., 2018. Observed rainfall trends and precipitation uncertainty in the vicinity of the Mediterranean, Middle East and North Africa. Theor. Appl. Clim. 134, 1207–1230. https://doi.org/10.1007/s00704-017-2333-0.

Zittis, G., Almazroui, M., Alpert, P., Ciais, P., Cramer, W., Dahdal, Y., Fnais, M., Francis, D., Hadjinicolaou, P., Howari, F., Jrrar, A., Kaskaoutis, D.G., Kulmala, M., Lazoglou, G., Mihalopoulos, N., Lin, X., Rudich, Y., Sciare, J., Stenchikov, G., Xoplaki, E., Lelieveld, J., 2022. Climate Change and Weather Extremes in the Eastern Mediterranean and Middle East. Rev. Geophys. 60, e2021RG000762. https://doi.org/10.1029/2021RG000762.

Zribi, L., Mouillot, F., Guibal, F., Rejeb, S., Rejeb, M.N., Gharbi, F., 2016. Deep soil conditions make Mediterranean cork oak stem growth vulnerable to autumnal rainfall decline in Tunisia. Forests 7, 245. https://doi.org/10.3390/f7100245.